

Theory of stochastic resonance in signal transmission by static nonlinear systems

François Chapeau-Blondeau and Xavier Godivier

Faculté des Sciences, Université d'Angers, 2 boulevard Lavoisier, 49000 Angers, France

(Received 1 July 1996; revised manuscript received 24 September 1996)

A deterministic periodic signal plus a stationary random noise is applied to a static nonlinearity taking the form of a monovariate arbitrary function on real numbers. The property of noise-enhanced signal transmission through stochastic resonance is studied for this class of static nonlinear systems. A theory is developed that provides expressions for the output autocorrelation function, power spectral density, signal-to-noise ratio, and input-output phase shift, in the presence of a periodic input, a noise distribution, and a static nonlinearity, all three being arbitrary. Both white and colored input noises are successively considered. For white input noise, exact expressions are derived in a discrete-time framework directly confrontable to simulations or experiments. The theory is applied to describe stochastic resonance in various examples of static nonlinear systems, for instance, a diode nonlinearity. In addition, confrontations with experiments and simulations are given that support the theory. In particular, interesting effects are reported such as a signal-to-noise ratio larger at the output than at the input or stochastic resonance at zero frequency. Finally, the validity of the theory is extended to dynamic nonlinear systems that can be decomposed into a static nonlinearity followed by an arbitrary dynamic linear system. [S1063-651X(97)12002-5]

PACS number(s): 05.40.+j, 02.50.-r, 07.50.Qx, 47.20.Ky

I. INTRODUCTION

Stochastic resonance is a nonlinear phenomenon whereby the transmission of a coherent (usually periodic) signal by certain nonlinear systems can be improved by noise addition in the system. This paradoxical nonlinear effect was first introduced in the domain of climate dynamics [1–3]. It has since been observed in a variety of both model and natural systems, including electronic circuits, lasers, electron paramagnetic resonance, a magnetoelastic pendulum, chemical reactions, superconducting devices, and neurons [4–8].

We specify that the stochastic resonance is here understood in a broad (modern) sense. It refers to an effect of noise-enhanced signal transmission that can be characterized by a signal-to-noise ratio (or another measure of the efficiency of the transmission) displaying a nonmonotonic evolution with the noise level and peaking at a maximum value for a sufficient noise level, whence we get the term “resonance.” In particular, the condition present at the origin, of a matching between a characteristic frequency belonging to the system with another one belonging to the external forcing, is no longer a requirement. Further developments have shown that the noise-enhanced signal transmission effect, referred to as “stochastic resonance,” is preserved over broader conditions that depart from that of a strict conventional resonance as in linear theory.

Several types of nonlinear systems have been shown to exhibit stochastic resonance [6,7,9,8]. The effect was originally observed in nonlinear dynamic systems governed by bistable, or, more generally multistable, potentials [2,3,10,11]. The stable states accessible to these systems are separated by potential barriers and the transitions between these stable states under the influence of the coherent signal plus the noise are monitored to observe stochastic resonance. Later, the works in [12–14] showed that multistability was not required (only nonlinearity), as they reported stochastic resonance in nonlinear dynamic systems governed by

monostable smooth single-well potentials. The effect was then extended to excitable systems [15–18], in which a noisy signal is compared to a threshold, the crossing of which triggers a deterministic excursion of the output before it returns to its resting state. The deterministic excursion of the output usually takes the form of a stereotypical pulse that is emitted each time the noisy input crosses the threshold, with possibly restrictions on the direction of the crossing. Recently, simple threshold systems in which the notion of a deterministic reset of the output of excitable systems has disappeared were also shown to be capable of stochastic resonance [19–22]. Here the state of the output, at any time, simply depends upon the position of the coherent input plus the noise relative to a threshold.

The nonlinear systems we shall consider in the present study can be viewed as an extension and generalization of these simple threshold systems, although some types of excitable systems will also be touched. Essentially, we shall consider nonlinear systems where a deterministic periodic signal plus a stationary random noise is applied to a static (or memoryless) nonlinearity taking the form of a monovariate arbitrary function on real numbers. Stochastic resonance will be demonstrated in various illustrative examples of static nonlinear systems of this type.

The theoretical description of stochastic resonant systems is made difficult by their nonlinear and nonstationary characters, and one usually has to resort to approximations. Frequent approximations are that of a slow and small periodic input signal and are often restricted to a Gaussian input noise. There have been several general approaches to the theoretical modeling of stochastic resonance (see [5,6,9,7,8] and references therein). As recently recognized in [8], it has now become difficult, in a limited space, to account for all the numerous theoretical methods by which stochastic resonance has been approached. We simply sketch, in the following, important seminal theories that have been developed for

the various types of stochastic resonant systems as mentioned above.

An important theory has been put forth [23] that essentially applies to bistable dynamic systems. This theory [23] is based on a rate equation determining the probability of occupation of the two stable states. In the limit of a small periodic input, this theory derives approximate expressions for the characteristics of the output that stochastically resonates. Also, for complete applicability, a requirement is an explicit expression for the transition rate between states, which is usually obtainable only within the approximation of a slow periodic input (adiabatic approximation) associated with a Gaussian noise, often under the form of a modified Kramers rate. For the bistable dynamic systems, with white noise, the approaches of [11,24] avoid the approximation of a slow periodic input and derive important properties of the stationary asymptotic behavior [11] and an expression of the output signal-to-noise ratio (SNR) valid for a small periodic input and weak noise [24]. These works [11,24] are based on the use of a Fokker-Planck equation that constitutes, in principle, a general approach to treat Markovian stochastic dynamics and characterize their second-order statistics required to analyze stochastic resonance. Yet, in this nonlinear context, a Fokker-Planck equation approach usually requires approximations for practical tractability, as carried out in [11,24].

The monostable nonlinear dynamic systems were approached in [13] by linear-response theory to analyze stochastic resonance. Linear-response theory is a perturbative method based on the linearization of the response of the system to a small periodic input when added to the noise. In principle, it can be applied to any nonlinear system [25–28] in the small-signal limit, and for this reason it offers a unifying framework for stochastic resonance in these conditions [9]. However, there is an important range where stochastic resonance occurs (when the signal is not small), which lies beyond the domain of applicability of linear-response theory [9]. Also, in practice, linear-response theory usually requires additional specific assumptions in order to make possible the explicit evaluation of a linear susceptibility, usually by means of the fluctuation-dissipation theorem in the presence of a thermal noise.

One type of excitable system has been theoretically analyzed in [17], with the adiabatic approximation to derive the output SNR for Gaussian input noise in the limit of a small periodic input. For the same system with Gaussian noise, the treatment in [18] avoids the approximation of a slow and small periodic input. For another type of excitable system, the analysis in [15], with Gaussian white input noise, imposes a Kramers-type formula to obtain an expression for the output SNR.

For the simple threshold systems, under the form of a single-threshold Heaviside nonlinearity, the model in [19] uses Gaussian white noise filtered by first-order or second-order low-pass linear filters. Expressions are then derived for the correlation functions and power spectral densities, allowing the characterization of the stochastic resonance by means of a correlation coefficient equivalent to the output SNR in the limit of a small periodic input. For the case of white noise (not necessarily Gaussian), the model in [22] derives an exact expression for the SNR with an arbitrary periodic

input. The works in [20,21] consider double-threshold or multithreshold systems and develop an approximate characterization of stochastic resonance.

Also, most of the aforementioned treatments deal with the transmission of a coherent signal under the form of a sinusoid. Stochastic resonance in the transmission of nonsinusoidal periodic signals has been considered only recently [29,22] and it finds interesting applications in the transmission of spike trains by neurons [30–32].

As mentioned, the type of static nonlinear system we shall consider here extends and generalizes the simple threshold systems and will also encompass a number of excitable systems. For such static nonlinear systems, we develop a complete theory for the characterization of stochastic resonance. This theory provides expressions for the output autocorrelation function, power spectral density, signal-to-noise ratio, and input-output phase shift, in the presence of a periodic input, a noise distribution, and a static nonlinearity, all three being arbitrary. Both white and colored input noise are successively considered. The theory does not resort to common adiabatic approximations nor Kramers-type formulations and is not restricted to small-signal or small-noise limits. Instead, it proceeds through a more direct statistical analysis made possible with static nonlinearities. Confrontations with experiments and simulations will be given. Finally, it will be established that the applicability of the theory extends to any dynamic nonlinear system that can be decomposed into a static nonlinearity followed by an arbitrary dynamic linear system. We have to specify that only periodic stochastic resonance (the most common type studied to date) is considered here and new forms of aperiodic stochastic resonance [33] will not be explicitly addressed here.

II. GENERAL FRAMEWORK FOR STOCHASTIC RESONANCE

We begin our analysis with the setting of a general framework for the description of stochastic resonance, which is generic and applies to any nonlinear system (static or dynamic). Elements of this framework have already been put in place, in other studies, in particular in [34,18], but usually with reference to specific nonlinear systems. We here set this framework in general form, with no reference to any particular nonlinear system. We shall then show, in the following sections, how this general formulation can be explicitly realized for static nonlinear systems.

Let $s(t)$ represent a periodic deterministic signal with period T_s and $\eta(t)$ a stationary random noise. We consider a time-invariant nonlinear system of general type (static or dynamic), which receives $s(t)$ and $\eta(t)$ as inputs and produces an output $y(t)$. We consider $y(t)$ as the steady-state response of the system or, in other words, we consider that the inputs $s(t)$ and $\eta(t)$ have been applied since $t \rightarrow -\infty$.

In general, because of the influence of the random input $\eta(t)$, the output $y(t)$ will be a random signal. Because of the influence of the deterministic input $s(t)$, the output $y(t)$ will be a nonstationary random signal. However, since $s(t)$ is periodic, $y(t)$ will in general be a cyclostationary random signal with period T_s [35].

At any time t , we express the random output signal $y(t)$ as the sum of its nonstationary mean $E[y(t)]$ plus the statis-

tical fluctuations $\tilde{y}(t)$ around the mean:

$$y(t) = \tilde{y}(t) + E[y(t)]. \quad (1)$$

Because of the cyclostationarity property of $y(t)$, the nonstationary mean $E[y(t)]$ is a deterministic periodic function of t with period T_s , for which we introduce the Fourier coefficients

$$\bar{Y}_n = \frac{1}{T_s} \int_0^{T_s} E[y(t)] \exp\left(-i2\pi \frac{n}{T_s} t\right) dt. \quad (2)$$

For the purpose of computing a statistical autocorrelation function for the output signal $y(t)$, we now consider for fixed t and τ the expectation

$$E[y(t)y(t+\tau)] = E[\tilde{y}(t)\tilde{y}(t+\tau)] + E[y(t)]E[y(t+\tau)]. \quad (3)$$

The expectation $E[y(t)y(t+\tau)]$ of Eq. (3) is a deterministic function of the two variables t and τ , which is periodic in t with period T_s . It is possible to construct a stationary (independent of t) autocorrelation function $R_{yy}(\tau)$ for $y(t)$ through a proper time averaging of $E[y(t)y(t+\tau)]$ over an interval T_s , when t , or $t \bmod T_s$, uniformly covers $[0, T_s[$, as

$$R_{yy}(\tau) = \frac{1}{T_s} \int_0^{T_s} E[y(t)y(t+\tau)] dt. \quad (4)$$

According to Eq. (3) one also has

$$R_{yy}(\tau) = C_{yy}(\tau) + \frac{1}{T_s} \int_0^{T_s} E[y(t)]E[y(t+\tau)] dt, \quad (5)$$

with the stationary autocovariance function of $y(t)$ defined as

$$C_{yy}(\tau) = \frac{1}{T_s} \int_0^{T_s} E[\tilde{y}(t)\tilde{y}(t+\tau)] dt. \quad (6)$$

We now define the power spectral density $P_{yy}(\nu)$ of $y(t)$ as the Fourier transform of the autocorrelation function $R_{yy}(\tau)$:

$$P_{yy}(\nu) = \mathcal{F}[R_{yy}(\tau)] = \int_{-\infty}^{+\infty} R_{yy}(\tau) \exp(-i2\pi\nu\tau) d\tau. \quad (7)$$

Fourier transforming Eq. (5) then leads to

$$P_{yy}(\nu) = \mathcal{F}[C_{yy}(\tau)] + \sum_{n=-\infty}^{+\infty} \bar{Y}_n \bar{Y}_n^* \delta\left(\nu - \frac{n}{T_s}\right). \quad (8)$$

The power spectral density of Eq. (8) has the typical form generically encountered with stochastic resonant systems. It is formed by spectral lines with magnitude $|\bar{Y}_n|^2$ at integer multiples of the coherent frequency $1/T_s$, superposed to a broadband noise background represented by $\mathcal{F}[C_{yy}(\tau)]$.

The autocovariance $E[\tilde{y}(t)\tilde{y}(t+\tau)]$ is expected to go to zero when $|\tau| \rightarrow +\infty$, and so is its time average $C_{yy}(\tau)$. $E[\tilde{y}(t)\tilde{y}(t)] = \text{var}[y(t)]$ represents the nonstationary variance of $y(t)$, which, after time averaging over a pe-

riod T_s according to Eq. (6), yields $C_{yy}(0) = \overline{\text{var}[y(t)]}$, the stationary variance of $y(t)$. The deterministic function $C_{yy}(\tau)$ can thus be written as

$$C_{yy}(\tau) = \overline{\text{var}[y(t)]} h(\tau), \quad (9)$$

where $h(\tau)$ is a deterministic even function describing the normalized shape of the stationary autocovariance; it verifies $h(0) = 1$ and $h(\tau) \rightarrow 0$ when $|\tau| \rightarrow +\infty$ and has a Fourier transform $\mathcal{F}[h(\tau)] = H(\nu)$. The power spectral density of Eq. (8) can then be expressed as

$$P_{yy}(\nu) = \overline{\text{var}[y(t)]} H(\nu) + \sum_{n=-\infty}^{+\infty} \bar{Y}_n \bar{Y}_n^* \delta\left(\nu - \frac{n}{T_s}\right). \quad (10)$$

A classical definition of the signal-to-noise ratio, at frequency n/T_s on the output, follows as the ratio of the power contained in the spectral line alone to the power contained in the noise background in a small frequency band ΔB around n/T_s . The corresponding expression of the output SNR is then

$$\mathcal{R}\left(\frac{n}{T_s}\right) = \frac{|\bar{Y}_n|^2}{\overline{\text{var}[y(t)]} H(n/T_s) \Delta B}. \quad (11)$$

Equation (11) provides an exact expression for the output SNR, whose explicit evaluation requires the knowledge of the nonstationary output mean $E[y(t)]$ and of the stationary output autocovariance function $C_{yy}(\tau)$.

Another desirable characterization of a stochastic resonant system consists in the possibility of evaluating the phase shift between the output and the coherent periodic input. This can be achieved through the computation of an input-output cross-correlation function. For fixed t and τ , we first consider the expectation

$$E[s(t)y(t+\tau)] = s(t)E[y(t+\tau)] \quad (12)$$

since $s(t)$ is deterministic.

$E[s(t)y(t+\tau)]$ is periodic in both t and τ , with period T_s . For the definition of a ‘‘stationary’’ cross-correlation function, a time average is taken when t , or $t \bmod T_s$, uniformly covers $[0, T_s[$. This yields the cross-correlation function

$$R_{sy}(\tau) = \frac{1}{T_s} \int_0^{T_s} s(t)E[y(t+\tau)] dt, \quad (13)$$

which is interpretable as the cross-correlation function of $s(t)$ with the nonstationary output mean $E[y(t)]$. $R_{sy}(\tau)$ of Eq. (13) is periodic with period T_s . Its frequency content has only components at integer multiples of $1/T_s$. Through a Fourier transform of $R_{sy}(\tau)$ similar to Eq. (7), one obtains a cross-power spectral density

$$P_{sy}(\nu) = \sum_{n=-\infty}^{+\infty} S_n \bar{Y}_n^* \delta\left(\nu - \frac{n}{T_s}\right), \quad (14)$$

where S_n , defined according to Eq. (2), is the order n Fourier coefficient of $s(t)$.

The phase shift ϕ between the mean output $E[y(t)]$ and the coherent input $s(t)$, as it is also considered in [26], can be evaluated, for a component with frequency n/T_s , from the argument of the complex number $P_{sy}(n/T_s)$ as

$$\phi\left(\frac{n}{T_s}\right) = \arg(S_n \bar{Y}_n^*). \quad (15)$$

The present framework shows how stochastic resonance, in any nonlinear system, can be fully characterized, especially the output SNR and input-output phase shift, from the sole knowledge of the nonstationary output mean $E[y(t)]$ over one period and of the stationary output autocovariance function $C_{yy}(\tau)$. We shall now use this framework as a guideline to study stochastic resonance in static nonlinearities.

III. STATIC NONLINEARITIES WITH WHITE NOISE

A. General model

The nonlinear system under consideration will now be a static (or memoryless) nonlinearity realizing the input-output transformation

$$y(t) = g[s(t) + \eta(t)], \quad (16)$$

where g is any function operating on real numbers, whose form will have to be further specified in order to obtain systems that exhibit stochastic resonance. As we shall see in the following, for the special case where $\eta(t)$ is a white noise, the general formulation of Sec. II can be explicitly realized and, moreover, in an exact way. We thus consider in Sec. III that $\eta(t)$ is a stationary white noise, although arbitrarily distributed, with the probability density function $f_\eta(u)$ and the statistical distribution function $F_\eta(u) = \int_{-\infty}^u f_\eta(u') du'$.

The autocorrelation function of the white noise is $R_{\eta\eta}(\tau) = E[\eta(t)\eta(t+\tau)] = 2D\delta(\tau)$ and, as a consequence, the white noise has an infinite power $E[\eta^2(t)] = R_{\eta\eta}(0)$. This singularity is a mark of the idealized character of the white noise. In practice, one has access only to approximations of a white noise, with a short but finite correlation time τ_c , a power $E[\eta^2(t)] = R_{\eta\eta}(0)$ that is large but finite, and verifying the condition $R_{\eta\eta}(0)\tau_c \sim 2D$.

We thus adopt such an embodiment for the input white noise $\eta(t)$ with a short but finite correlation time τ_c . Now, to have the possibility of a direct numerical evaluation of every relevant quantity of the model, especially for the purpose of comparison with simulations or experimental implementations of the nonlinear systems, we choose to move to the context of discrete-time signals. The time scale is thus discretized with a step $\Delta t \ll T_s$ such that $T_s = N\Delta t$. In practice now, the white noise $\eta(t)$ only needs to be a noise with a correlation time τ_c shorter than Δt and a finite power $E(\eta^2) = \sigma_\eta^2$. Such a noise, when sampled every Δt , implements the discrete-time white noise $\eta(t = j\Delta t)$ endowed with the autocorrelation function $R_{\eta\eta}(k\Delta t) = E[\eta(j\Delta t)\eta(j\Delta t + k\Delta t)] = \sigma_\eta^2 \Delta t \hat{\delta}(k\Delta t)$, with the discrete-time version of the Dirac delta function defined as

$$\hat{\delta}(k\Delta t) = \begin{cases} 1/\Delta t & \text{for } k=0 \\ 0 & \text{for } k \neq 0. \end{cases} \quad (17)$$

In this realization of the white noise, the power density is given by

$$2D = \sigma_\eta^2 \Delta t. \quad (18)$$

Now, in this discrete-time framework, the treatment that will follow is exact.

To proceed, we notice that a key simplification with a *white* noise $\eta(t)$ and a *static* nonlinearity $g(u)$ is that for any fixed t and any fixed $\tau \neq 0$, $y(t)$ and $y(t+\tau)$ are statistically uncorrelated, just as $\eta(t)$ and $\eta(t+\tau)$ are. As a consequence, the expectations on the output, in the discrete-time framework, verify

$$E[y(j\Delta t)y(j\Delta t + k\Delta t)] = E[y(j\Delta t)]E[y(j\Delta t + k\Delta t)] \quad (19)$$

for any integers j and $k \neq 0$. Only for the case $\tau = k\Delta t = 0$ one has

$$\begin{aligned} E[y(j\Delta t)y(j\Delta t)] &= E[\tilde{y}^2(j\Delta t)] + E^2[y(j\Delta t)] \\ &\neq E^2[y(j\Delta t)]. \end{aligned} \quad (20)$$

At any fixed time $t = j\Delta t$, since $\eta(t)$ is distributed according to $f_\eta(u)$, then $s(t) + \eta(t)$ is distributed according to $f_\eta[u - s(t)]$. As a result of the functional relationship (16), the nonstationary output mean can then be explicitly computed as

$$E[y(t)] = \int_{-\infty}^{+\infty} g(u) f_\eta[u - s(t)] du \quad (21)$$

and the nonstationary output degree-two moment as

$$E[y^2(t)] = \int_{-\infty}^{+\infty} g^2(u) f_\eta[u - s(t)] du. \quad (22)$$

An expression is then accessible for the nonstationary output variance $E[\tilde{y}(t)\tilde{y}(t)] = \text{var}[y(t)]$, as

$$\begin{aligned} \text{var}[y(t)] &= \int_{-\infty}^{+\infty} g^2(u) f_\eta[u - s(t)] du \\ &\quad - \left(\int_{-\infty}^{+\infty} g(u) f_\eta[u - s(t)] du \right)^2. \end{aligned} \quad (23)$$

Equations (19) and (20) can be combined into a single expression, in which every term is now explicitly known from Eqs. (21) and (23) and reads

$$\begin{aligned} E[y(j\Delta t)y(j\Delta t + k\Delta t)] &= \text{var}[y(j\Delta t)] \Delta t \hat{\delta}(k\Delta t) \\ &\quad + E[y(j\Delta t)]E[y(j\Delta t + k\Delta t)] \end{aligned} \quad (24)$$

for any integers j and k and $\hat{\delta}(k\Delta t)$ defined by Eq. (17). Through a time average, we then define the output autocorrelation function, in the discrete-time framework, corresponding to Eq. (4), as

$$R_{yy}(k\Delta t) = \overline{\text{var}(y)\Delta t \hat{\delta}(k\Delta t)} + \frac{1}{N} \sum_{j=0}^{N-1} E[y(j\Delta t)] \times E[y(j\Delta t + k\Delta t)], \quad (25)$$

with the stationary output variance

$$\overline{\text{var}(y)} = \frac{1}{N} \sum_{j=0}^{N-1} \text{var}[y(j\Delta t)], \quad (26)$$

which is explicitly computable from Eq. (23). The stationary output autocovariance function of Eq. (9) is then simply, for the case of white input noise and static nonlinearities,

$$C_{yy}(k\Delta t) = \overline{\text{var}(y)\Delta t \hat{\delta}(k\Delta t)} = \overline{\text{var}(y)}h(k\Delta t). \quad (27)$$

In order to proceed into the frequency domain, the Fourier coefficients of the deterministic periodic signal $E[y(j\Delta t)]$ are introduced as

$$\bar{Y}_n = \frac{1}{N} \sum_{j=0}^{N-1} E[y(j\Delta t)] \exp\left(-i2\pi \frac{jn}{N}\right). \quad (28)$$

The discrete Fourier transform of R_{yy} , over a time interval of an integer number $2M$ of periods T_s , is defined as

$$\mathcal{F}_{\text{dis}}[R_{yy}(k\Delta t)] = \sum_{k=-MN}^{MN-1} R_{yy}(k\Delta t) \exp\left(-i2\pi \frac{kl}{2MN}\right) \Delta t, \quad (29)$$

which affords a frequency resolution $\Delta\nu = 1/(2MN\Delta t)$.

The autocorrelation function of Eq. (25) is formed by a pulse at the origin with magnitude $\text{var}(y)\Delta t$, superposed to a periodic component with period T_s [the second term on the right-hand side of Eq. (25)]. The Fourier transform of R_{yy} defines the output power spectral density P_{yy} , which will then be formed by a constant background with magnitude $\text{var}(y)\Delta t$, superposed to a series of spectral lines at integer multiples of $1/T_s$. Application of Eq. (29) leads to

$$P_{yy}\left(\frac{n}{T_s}\right) = \overline{\text{var}(y)\Delta t} + \bar{Y}_n \bar{Y}_n^* \frac{1}{\Delta\nu}. \quad (30)$$

Because of condition (18), the quantity $\overline{\text{var}(y)\Delta t}$ is expected to remain finite. When the horizon $M \rightarrow +\infty$, then $\Delta\nu \rightarrow 0$ and the coherent spectral lines above the broadband noise background tend to Dirac δ pulses. This is the typical form of the power spectral density for the output of a stochastic resonant system. It comes here in Eq. (30) under a form appropriate for direct numerical evaluation.

Since the function $h(\tau)$ is here simply $\Delta t \hat{\delta}(k\Delta t)$, its discrete Fourier transform is $H(\nu) = \Delta t \forall \nu$. The SNR of Eq. (11) follows as

$$\mathcal{R}\left(\frac{n}{T_s}\right) = \frac{|\bar{Y}_n|^2}{\overline{\text{var}(y)\Delta t \Delta B}}. \quad (31)$$

The output SNR of Eq. (31) is then completely calculable, through Eqs. (21), (28), (23), and (26) for any noise distribution $f_\eta(u)$ and any periodic input $s(t)$ transmitted through an arbitrary nonlinearity $g(u)$. The input-output phase shift

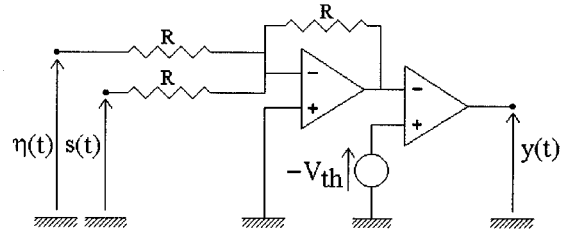


FIG. 1. Experimental electronic circuit implementing the non-linearity of Eq. (33).

ϕ of Eq. (15) is also completely calculable, in the discrete-time framework, with the Fourier coefficient S_n evaluated through an equation similar to Eq. (28).

With the SNR and phase shift ϕ , both accessible at the different harmonics of the coherent frequency $1/T_s$, we have a complete characterization of the nonlinear system that is suited to detect a stochastic resonance effect, with the relevant quantities lending themselves to direct numerical evaluation. The following illustrates the capability of the present theory to analyze stochastic resonance in various examples of static nonlinear systems.

B. Experimental test

The work in [22] considers a special case of the present general treatment, when the nonlinearity $g(u)$ is a Heaviside function

$$g(u) = \begin{cases} 0 & \text{for } u \leq \theta \\ 1 & \text{for } u > \theta. \end{cases} \quad (32)$$

Numerical simulations of stochastic resonance in this system are performed in [22] and compared to the theoretical predictions. The results show complete agreement.

It is also possible to experimentally implement a simple nonlinear system belonging to the class of the static stochastic resonators considered here. We achieved this with the electronic circuit with two operational amplifiers of Fig. 1. The circuit of Fig. 1 behaves as a two-state comparator with threshold V_{th} implementing a nonlinearity $g(u)$ of the form (with $V_{sat} > 0$)

$$g(u) = \begin{cases} -V_{sat} & \text{for } u < V_{th} \\ +V_{sat} & \text{for } u > V_{th}. \end{cases} \quad (33)$$

One may note that the nonlinear circuit of Fig. 1 possesses only a threshold nonlinearity and falls in the class of static, or memoryless, nonlinear systems. It has to be contrasted with another nonlinear electronic circuit, a Schmitt trigger, also shown to exhibit stochastic resonance [36]. The Schmitt trigger possesses both a threshold and hysteretic nonlinearity and falls in the class of dynamic nonlinear systems, or systems with memory, because of the hysteresis.

A detailed study of stochastic resonance in the circuit of Fig. 1 will be given elsewhere [37]. For the nonlinearity of Eq. (33), Eq. (21) of the general model of Sec. III A yields

$$E[y(t)] = V_{sat} \{1 - 2F_\eta[V_{th} - s(t)]\} \quad (34)$$

and Eq. (23) yields

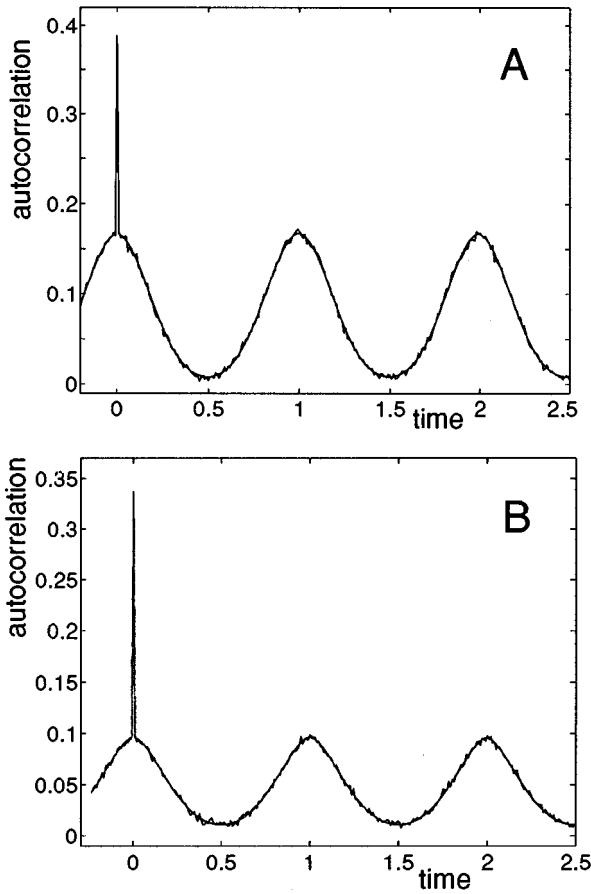


FIG. 2. Output autocorrelation function $R_{yy}(\tau)$ in units V_{sat}^2 as a function of the time lag τ in units T_s , for the two-state threshold comparator with a zero-mean Gaussian input white noise $\eta(t)$. (A) Sinusoid $s(t) = V_M \sin(2\pi t/T_s)$ and (B) triangular wave $s(t) = V_M s_1(t/T_s)$ from Eq. (36). The signal amplitude is $V_M = 1.9$ V, the threshold $V_{\text{th}} = 2.2$ V, and the input noise rms amplitude is here 1.4 V. The smooth line is the theoretical expression from Eqs. (25), (34), and (35); the noisy line (almost indistinguishable) is the experimental estimation on the circuit of Fig. 1.

$$\text{var}[y(t)] = 4V_{\text{sat}}^2 \{1 - F_{\eta}[V_{\text{th}} - s(t)]\} F_{\eta}[V_{\text{th}} - s(t)]. \quad (35)$$

For illustration, Fig. 2 shows the output autocorrelation function $R_{yy}(\tau)$ theoretically computed from Eqs. (25), (34), and (35), compared with an experimental estimation of $R_{yy}(\tau)$, obtained with $\Delta t = T_s/N$, $N = 100$, the period $T_s = 10$ ms, the noise $\eta(t)$ zero-mean Gaussian, and the periodic input being successively a sinusoid $s(t) = V_M \sin(2\pi t/T_s)$ and a triangular wave $s(t) = V_M s_1(t/T_s)$, with the zero-mean symmetric normalized triangular wave

$$s_1(t) = \begin{cases} 1 - 4t & \text{for } 0 \leq t < \frac{1}{2} \\ -3 + 4t & \text{for } \frac{1}{2} \leq t < 1, \end{cases} \quad (36)$$

and $s_1(t)$ with period 1. The output autocorrelation function $R_{yy}(\tau)$ was experimentally estimated on the circuit of Fig. 1 by averaging products $y(t)y(t+\tau)$, with values of $t \bmod T_s$ uniformly covering the interval $[0, T_s]$ for every value of τ at which $R_{yy}(\tau)$ was estimated. The theory of Sec. III A in the

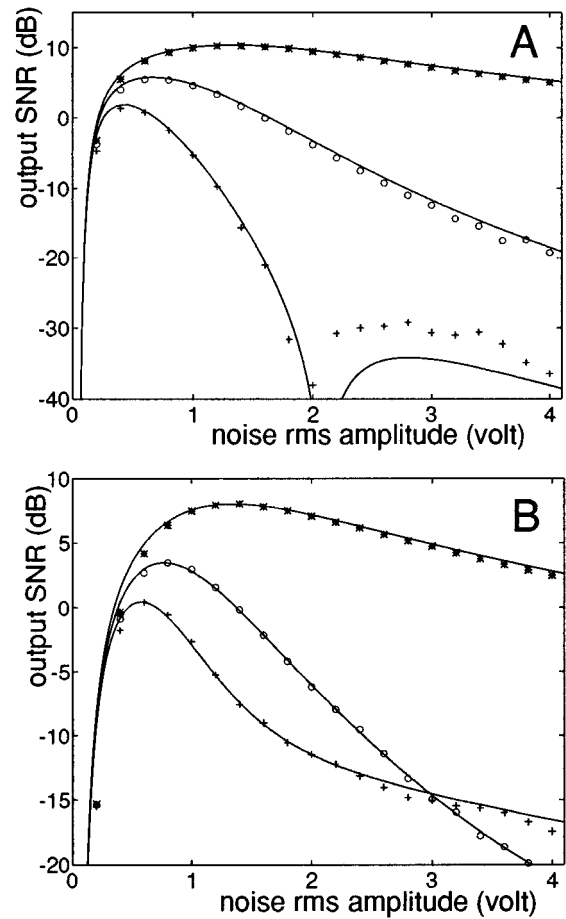


FIG. 3. Output signal-to-noise ratio \mathcal{R} in decibels, as a function of the rms amplitude in volts of the input white noise $\eta(t)$ chosen to be zero-mean Gaussian, for the two-state threshold comparator. (A) Sinusoid $s(t) = V_M \sin(2\pi t/T_s)$ and (B) triangular wave $s(t) = V_M s_1(t/T_s)$ from Eq. (36). The signal amplitude is $V_M = 1.9$ V and the threshold $V_{\text{th}} = 2.2$ V. In each panel the solid line is the theoretical expression from Eqs. (31), (34), and (35) and the sets of discrete data points were experimentally obtained with the circuit of Fig. 1. In each panel, the SNR is shown at the fundamental frequency $1/T_s$ and at the two subsequent harmonics n/T_s that give the strongest SNR: at $1/T_s$ (*), at $2/T_s$ (O), and at $3/T_s$ (+).

discrete-time framework is exact and the very same expressions are evaluated in the theoretical analysis and in the experiment. Consequently, as expected, Fig. 2 shows very good agreement between the theoretical and experimental autocorrelation functions and both would tend to perfectly superpose if the averages in the experiment were performed with a number of samples tending to infinity.

Application of Eqs. (28) and (26) with Eqs. (34) and (35) allows the explicit evaluation of the theoretical output SNR of Eq. (31). We chose (arbitrarily) a band $\Delta B = 1/T_s = 1/(N\Delta t)$, with $N = 100$, and we shall stick to these values for the rest of the article. Figure 3 represents the SNR theoretically computed from Eq. (31), compared with the SNR experimentally measured from the circuit of Fig. 1, successively with the sinusoid $s(t) = V_M \sin(2\pi t/T_s)$ and the triangular wave $s(t) = V_M s_1(t/T_s)$ from Eq. (36). The nonmonotonic evolutions of the SNRs in Fig. 3 present the signature of stochastic resonance: the SNRs peak at a maximum

value for a sufficient level of the input noise and there exists a range where increasing the input noise results in a higher output SNR. The comparison of the SNRs of Fig. 3 shows again the same very good agreement between theory and experiment, up to very small values of the SNR close to the limit of accuracy of the measurements.

C. Two-threshold nonlinearity

A special instance of a static nonlinear system exhibiting stochastic resonance has been considered in [20] under the form of the two-threshold nonlinearity

$$g(u) = \begin{cases} -1 & \text{for } u < -0.5 \\ 0 & \text{for } -0.5 \leq u \leq 0.5 \\ 1 & \text{for } u > 0.5. \end{cases} \quad (37)$$

Equation (21) of the general model yields in this case

$$E[y(t)] = 1 - F_\eta[0.5 - s(t)] - F_\eta[-0.5 - s(t)] \quad (38)$$

and Eq. (23) yields

$$\begin{aligned} \text{var}[y(t)] = & \{1 - F_\eta[0.5 - s(t)]\} F_\eta[0.5 - s(t)] \\ & + \{1 - F_\eta[-0.5 - s(t)]\} F_\eta[-0.5 - s(t)] \\ & + 2\{1 - F_\eta[0.5 - s(t)]\} F_\eta[-0.5 - s(t)]. \end{aligned} \quad (39)$$

From Eqs. (38) and (39), application of Eqs. (28) and (26) leads to an explicit expression for the SNR of Eq. (31). Figure 4 represents this SNR of the stochastic resonator of Eq. (37), computed again with $\Delta B = 1/T_s = 1/(N\Delta t)$ and $N = 100$, for different noise distributions and two different wave forms for the periodic input, a sinusoid $s(t) = A \sin(2\pi t/T_s)$ and a sawtooth $s(t) = A s_2(t/T_s)$, with

$$s_2(t) = -1 + 2(t \bmod 1). \quad (40)$$

The conventional SNR appearing in Fig. 4 is not computed in the study of [20]. Instead, in [20], the stochastic resonance effect in the transmission by Eq. (37) is characterized by means of the amplitude of the coherent spectral line at frequency $1/T_s$ on the output. One may note, however, that such a quantity does not provide a strict assurance of the presence of stochastic resonance, because when the input noise level is raised, both the coherent line and the noise background may simultaneously increase at the output (see Fig. 6), while a preferable requirement is a coherent line whose relative emergence out of the noise background becomes more pronounced. The amplitude of the output coherent line at $1/T_s$ used in [20] corresponds to our $|\bar{Y}_1|$ from Eq. (28). No comparable general expression is offered for this quantity in [20], yet when $s(t) = A \sin(2\pi t/T_s)$ this quantity is approximated in [20] as kA_y , with

$$A_y = F_\eta(0.5 + A) - F_\eta(0.5 - A) \quad (41)$$

and k an *ad hoc* proportionality constant.

Figure 5 compares the approximation kA_y from Eq. (41) with the value $|\bar{Y}_1|$ from Eqs. (28) and (38). As noted in [20], the approximation kA_y is good for small values of A , and we

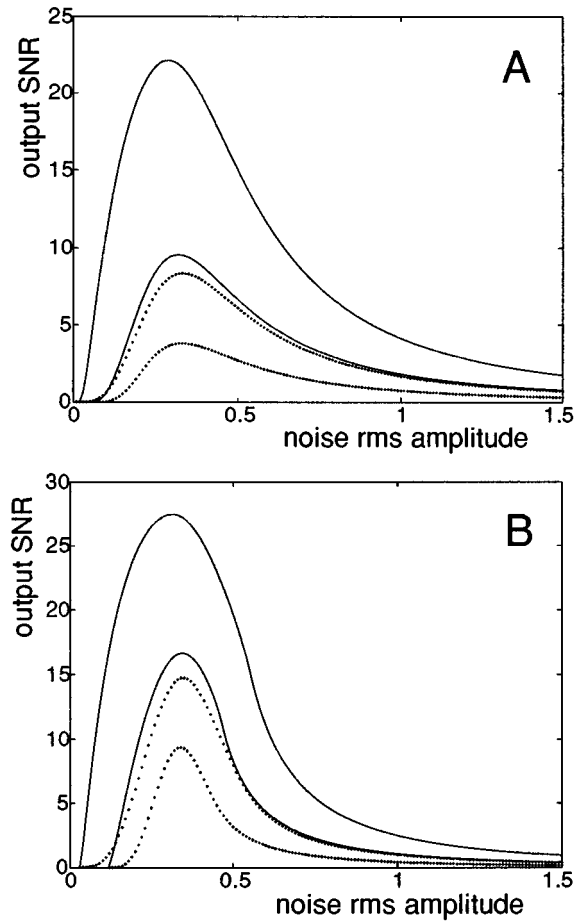


FIG. 4. Output signal-to-noise ratio \mathcal{R} at frequency $1/T_s$ computed from Eqs. (31), (38), and (39) for the two-threshold nonlinearity of Eq. (37), as a function of the rms amplitude of the input white noise $\eta(t)$. (A) $\eta(t)$ a zero-mean Gaussian noise and (B) $\eta(t)$ a zero-mean uniform noise. In each panel, the pair of solid curves is with a sinusoidal $s(t) = A \sin(2\pi t/T_s)$ and the pair of dotted curves with a sawtooth $s(t) = A s_2(t/T_s)$ from Eq. (40). In each pair, the upper curve is with $A = 0.45$ and the lower curve with $A = 0.3$.

can see in Fig. 5 that it degrades for larger A 's. Also, as mentioned in [20], the approximation ignores the actual shape of the periodic input $s(t)$ and as is visible in Fig. 5, the discrepancy is increased when $s(t)$ is changed from a sinusoid to a sawtooth.

The present theory has also the ability to describe stochastic resonance in multithreshold systems as considered in [21] and to predict the SNRs that are approximated in the study of [21]. We can also illustrate, with the two-threshold nonlinearity of Eq. (37), the evolution of the output stationary variance $\text{var}(y)$ from Eqs. (26) and (23), which controls the noise background in the SNR of Eq. (31). This evolution of $\text{var}(y)$ with the rms amplitude of the input noise $\eta(t)$ is represented in Fig. 6 in the presence of a periodic input $s(t) = A \sin(2\pi t/T_s)$ with $A = 0.45$ and also, for comparison, in the absence of any periodic input. From Fig. 6, it is visible that in the region of the resonance, the output noise background may differ significantly in the presence of the periodic input from its value in the absence of this periodic input. This is the case here, where the amplitude $A = 0.45$ of the periodic input is of the same order of magnitude as the

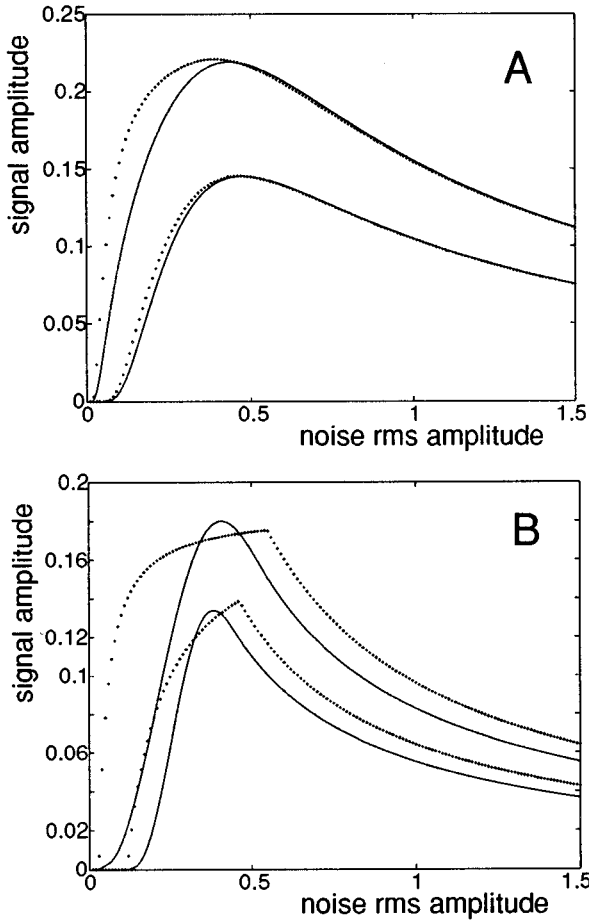


FIG. 5. Amplitude of the coherent spectral line at frequency $1/T_s$ on the output of the two-threshold nonlinearity of Eq. (37), as a function of the rms amplitude of the input white noise $\eta(t)$. (A) $\eta(t)$ a zero-mean Gaussian noise, a sinusoidal input $s(t) = A \sin(2\pi t/T_s)$, and $k=0.50$. (B) $\eta(t)$ a zero-mean uniform noise, a sawtooth input $s(t) = A s_2(t/T_s)$ from Eq. (40), and $k=0.37$. In each panel, the pair of solid curves is the exact expression given by $|\bar{Y}_1|$ from Eqs. (28) and (38) and the pair of dotted curves is the approximation kA_y from Eq. (41) after [20]. In each pair, the upper curve is with $A=0.45$ and the lower curve with $A=0.3$.

characteristic amplitudes in the system [the threshold 0.5 in Eq. (37) and the noise rms amplitude of around 0.3 at the peak of the resonance]. Under these conditions, the periodic input cannot be considered small and its implication in stochastic resonance cannot be treated accurately if the noise background in the presence of the periodic input is simply replaced by this background in its absence. This is what would have been assumed in a perturbative treatment of stochastic resonance, yet efficient in its own domain of applicability. Perturbative treatments, such as linear-response theory [25,26], are general in the sense that they can be applied to any nonlinear systems, but they are restricted to the small-signal limit. In contrast, our present approach applies only to static nonlinearities, but for this type of system it provides a general description, not restricted to the small-signal limit. The conditions illustrated in Fig. 6 lead us here to view stochastic resonance not as a perturbative effect, but as a truly cooperative effect in which two signals with comparable im-

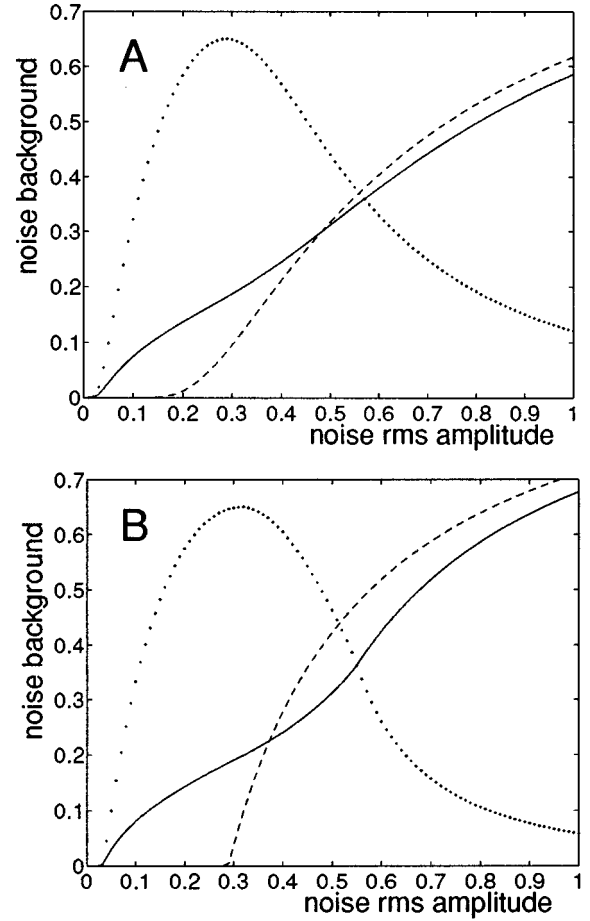


FIG. 6. Output noise background $\overline{\text{var}(y)}$ from Eqs. (26), (23), and (39), which controls the denominator of the SNR of Eq. (31) for the two-threshold nonlinearity of Eq. (37), as a function of the rms amplitude of the input white noise $\eta(t)$. (A) $\eta(t)$ a zero-mean Gaussian noise and (B) $\eta(t)$ a zero-mean uniform noise. In each panel, the solid curve is $\overline{\text{var}(y)}$ in the presence of the periodic input $s(t) = A \sin(2\pi t/T_s)$ with $A=0.45$ and the dashed curve is $\overline{\text{var}(y)}$ in the absence of any periodic input. To locate the resonance, we have redrawn (dotted curves) the corresponding SNRs from Fig. 4 after normalization of their maximum value to 0.65 to fit adequately in the figure.

portance (no one dominates the other), a periodic one and a noise, efficiently cooperate to overcome a nonlinearity.

D. Diodelike nonlinearity

As another application of the present theory, we now examine the case where

$$g(u) = \begin{cases} 0 & \text{for } u \leq \theta \\ (u - \theta)/\lambda & \text{for } u > \theta. \end{cases} \quad (42)$$

Equation (42) is a simple model for the nonlinearity of a diode with threshold θ . The diode is one of the most elementary nonlinear electronic components. With the present theory, we can verify that this component, with the model of Eq. (42), is capable of stochastic resonance.

Following the procedure of Sec. III A, we computed with the nonlinearity (42) the output SNR of Eq. (31). This was performed with $\eta(t)$ a zero-mean Gaussian noise with vari-

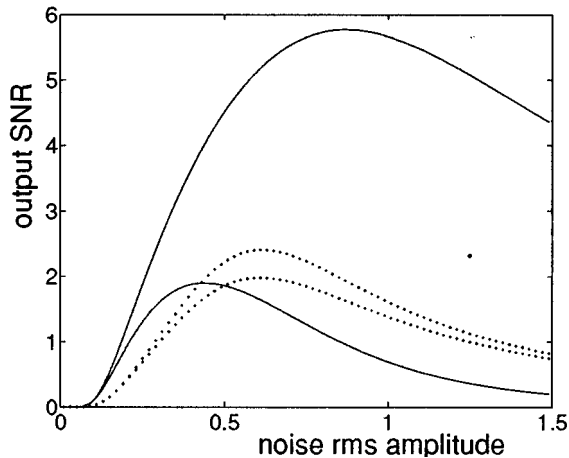


FIG. 7. Output signal-to-noise ratio \mathcal{R} computed from Eq. (31) for the diode nonlinearity of Eq. (42) with $\theta=1.2$, as a function of the rms amplitude σ_η of the input white noise $\eta(t)$ chosen to be zero-mean Gaussian. The pair of solid curves is with $s(t)=\cos(2\pi t/T_s)$ and the pair of dotted curves with $s(t)=[\cos(2\pi t/T_s)+\cos(4\pi t/T_s+\pi/4)+\cos(6\pi t/T_s+2\pi/5)]/3$. In each pair, the upper curve is the SNR at frequency $1/T_s$ and the lower curve the SNR at $2/T_s$.

ance σ_η^2 and a threshold $\theta=1.2$. For illustration, the periodic input of period T_s was successively $s(t)=\cos(2\pi t/T_s)$ and $s(t)=[\cos(2\pi t/T_s)+\cos(4\pi t/T_s+\pi/4)+\cos(6\pi t/T_s+2\pi/5)]/3$. The resulting SNRs, plotted in Fig. 7 as a function of the rms amplitude σ_η of the noise $\eta(t)$, reveal stochastic resonance in the diode nonlinearity. The SNR predicted by Eq. (31) is insensitive to the value of the parameter λ of Eq. (42). As visible in Fig. 7, no linear superposition applies since we are dealing with nonlinear systems and the behavior of the SNR for the component at frequency $1/T_s$ is different whether this component is alone or accompanied by other components with different frequencies. Also visible in Fig. 7, as well as in Fig. 3, a single harmonic input at frequency $1/T_s$ has the ability to generate higher-order harmonics at the output, since the context is nonlinear.

We can also illustrate, with the diode nonlinearity of Eq. (42), the evolution of the input-output phase shift of Eq. (15). For the diode nonlinearity of Eq. (42) with the Gaussian noise $\eta(t)$, application of Eq. (21) leads to

$$E[y(t)] = \frac{\sigma_\eta}{\lambda\sqrt{2\pi}} \left\{ \exp[-z_1^2(t)] - \sqrt{\pi}z_1(t)\text{erfc}[z_1(t)] \right\}, \quad (43)$$

with $z_1(t)=[\theta-s(t)]/(\sigma_\eta\sqrt{2})$.

The resulting input-output phase shift of Eq. (15) is represented in Fig. 8 as a function of the rms amplitude σ_η of the Gaussian noise $\eta(t)$. Three different periodic inputs $s(t)$ with the same period T_s were successively applied in order to illustrate the rich variability of the evolution of the input-output phase shift with stochastic resonance in static nonlinearities. First, with $s(t)=\cos(2\pi t/T_s)$, the present theory gives a phase shift $\phi(1/T_s)=0$ for any noise rms amplitude σ_η . Second, we continued with the addition of a harmonic at frequency $2/T_s$ at the input, with $s(t)=[\cos(2\pi t/T_s)+\cos(4\pi t/T_s+\pi/4)]/2$. As a result, the phase shift $\phi(1/T_s)$,

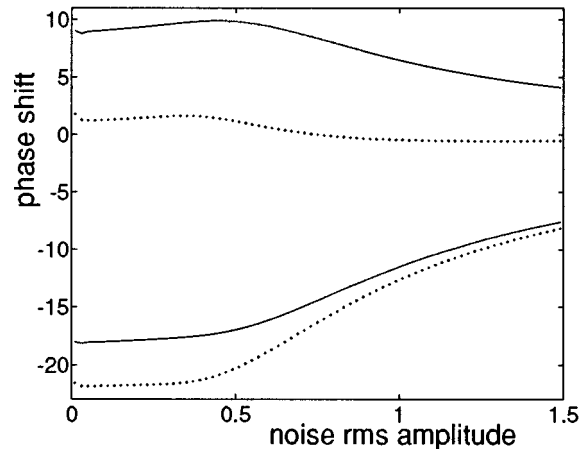


FIG. 8. Input-output phase shift ϕ (in degrees) computed from Eqs. (15) and (43) for the diode nonlinearity of Eq. (42) in the stochastic resonance regime of Fig. 7 with $\theta=1.2$, as a function of the rms amplitude σ_η of the Gaussian input white noise $\eta(t)$. The pair of solid curves is with $s(t)=[\cos(2\pi t/T_s)+\cos(4\pi t/T_s+\pi/4)]/2$ and the pair of dotted curves with $s(t)=[\cos(2\pi t/T_s)+\cos(4\pi t/T_s+\pi/4)+\cos(6\pi t/T_s+2\pi/5)]/3$. In each pair, the upper curve is ϕ at frequency $1/T_s$ and the lower curve ϕ at $2/T_s$.

between the input and output components at the frequency $1/T_s$ of the fundamental, experienced a dramatic change, as depicted in Fig. 8. Third, we further added a harmonic at frequency $3/T_s$ at the input, with $s(t)=[\cos(2\pi t/T_s)+\cos(4\pi t/T_s+\pi/4)+\cos(6\pi t/T_s+2\pi/5)]/3$. Again, as visible in Fig. 8, the phase shift $\phi(1/T_s)$ at the fundamental was further changed and also changed the phase shift $\phi(2/T_s)$ at the second harmonic.

The results of Fig. 8 illustrate typical properties that can be observed for the phase shift of Eq. (15). Nonzero input-output phase shifts can occur in stochastic resonance with static nonlinearities. The phase shift at a given frequency is strongly dependent upon the overall frequency content of the coherent input $s(t)$, since adding higher harmonics $2/T_s, 3/T_s, \dots$ at the input can change the phase shift of the component at the fundamental $1/T_s$. Such a behavior of the phase shift is a typical nonlinear property, which is absent in linear systems. Monotonic or nonmonotonic evolutions of the phase shift with the noise rms amplitude can be observed (see also [22]). Also, the present theory predicts that the input-output phase shift of Eq. (15), for a given periodic input $s(t)$, is influenced by the distribution of the input noise $\eta(t)$.

E. Nonsubliminal periodic input

It is interesting to examine the case where $g(u)$ is a smooth nonlinearity, monotonically increasing from 0 to 1, with the sigmoidal form

$$g(u) = \frac{1}{1 + \exp\left(-\frac{u-\theta}{\lambda}\right)}. \quad (44)$$

The parameter λ of Eq. (44) measures the extension of the

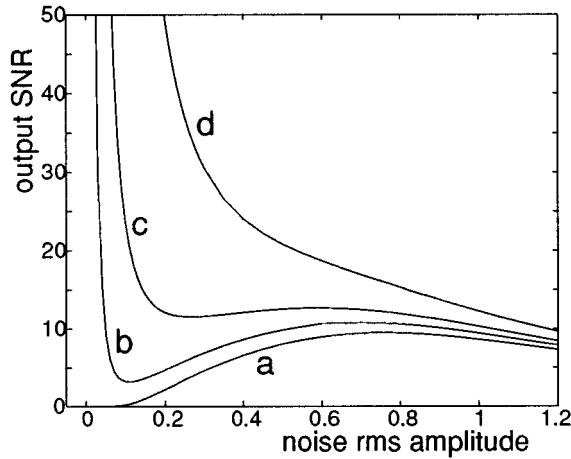


FIG. 9. Monotonic smooth nonlinearity. Output signal-to-noise ratio \mathcal{R} at frequency $1/T_s$ computed from Eq. (31) for the sigmoid nonlinearity of Eq. (44) with $\theta=1.2$, as a function of the rms amplitude of the input white noise $\eta(t)$ chosen to be zero-mean Gaussian. The periodic input is $s(t)=\cos(2\pi t/T_s)$. *a*, $\lambda=0$; *b*, $\lambda=0.05$; *c*, $\lambda=0.1$; and *d*, $\lambda=0.2$.

region around θ over which $g(u)$ passes from 0 to 1. As $\lambda \rightarrow 0$, this nonlinearity approaches the Heaviside function of Eq. (32).

With the procedure of Sec. III A, we computed for the nonlinearity (44) the SNR of Eq. (31). This was performed with $\eta(t)$ a zero-mean Gaussian noise, the periodic input $s(t)=\cos(2\pi t/T_s)$, and a threshold $\theta=1.2$. The resulting SNR is plotted in Fig. 9 as a function of the rms amplitude of the noise $\eta(t)$ and for different values of the “smoothness” λ of the nonlinearity (44).

For $\lambda=0$, the nonlinearity $g(u)$ reduces to the Heaviside function and the periodic input $s(t)$ alone is strictly subliminal, unable to induce any transition of the output in the absence of the noise. Then, an increase of the input noise level from zero produces a conventional stochastic resonance, as shown in Fig. 9(a), where the SNR increases from zero up to a maximum and then back down toward zero. For $\lambda>0$, $g(u)$ is a smooth nonlinearity and the periodic input $s(t)$ is visible at the output in the absence of the noise. Then, for a strictly zero input noise level, the output SNR tends to infinity. As the input noise level is increased above zero, for a steep $g(u)$ with small $\lambda>0$, we observe in Fig. 9 that the output SNR can rapidly drop to small values, from where a further increase of the noise level progressively raises the SNR as in a conventional stochastic resonance. For smoother $g(u)$ with larger λ the resonance disappears to give way to a monotonic decay of the SNR as the noise level is increased from zero.

The results of Fig. 9 demonstrate that a smooth nonlinearity can stochastically resonate, provided it contains parts with sufficient steepness. The presence of a strict threshold (below which the output is strictly unresponsive) is not necessary to obtain the possibility of a noise enhancement of the transmission. Figure 9 shows an example where a nonsubliminal coherent signal $s(t)$ corrupted by a small amount of noise can benefit from further noise addition to improve its transmission.

A similar type of resonance can also be obtained with nonmonotonic smooth nonlinearities, for instance a Gaussian one:

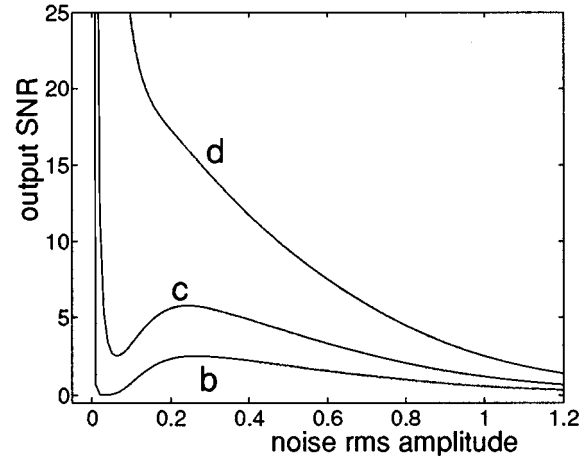


FIG. 10. Nonmonotonic smooth nonlinearity. Output signal-to-noise ratio \mathcal{R} at frequency $1/T_s$ computed from Eqs. (31), (46), and (47), for the Gaussian nonlinearity of Eq. (45) with $\theta=1.2$, as a function of the rms amplitude of the zero-mean Gaussian input white noise $\eta(t)$. The periodic input is $s(t)=\cos(2\pi t/T_s)$. *b*, $\lambda=0.05$; *c*, $\lambda=0.1$; and *d*, $\lambda=0.2$.

$$g(u) = \exp\left[-\left(\frac{u-\theta}{\lambda}\right)^2\right]. \quad (45)$$

For this nonlinearity of Eq. (45), with a zero-mean Gaussian input noise $\eta(t)$ of variance σ_η^2 , an explicit analytical expression can be written for Eq. (21) in the form

$$E[y(t)] = \left[\left(\frac{\sigma_\eta \sqrt{2}}{\lambda} \right)^2 + 1 \right]^{-1/2} \exp[-z_2(t)], \quad (46)$$

with

$$z_2(t) = \left[\frac{s(t)}{\sigma_\eta \sqrt{2}} \right]^2 + \left(\frac{\theta}{\lambda} \right)^2 - \left[\left(\frac{\sigma_\eta \sqrt{2}}{\lambda} \right)^2 + 1 \right]^{-1} \times \left[\frac{s(t)}{\sigma_\eta \sqrt{2}} + \frac{\sigma_\eta \sqrt{2}}{\lambda} \frac{\theta}{\lambda} \right]^2. \quad (47)$$

Then, substitution of λ by $\lambda/\sqrt{2}$ in Eqs. (46) and (47) simply yields the explicit expression for $E[y^2(t)]$ of Eq. (22), leading to the SNR of Eq. (31) depicted in Fig. 10. The results of Fig. 10 demonstrate that a nonmonotonic smooth nonlinearity, with sufficiently steep parts, can also stochastically resonate.

F. Influence of the noise distribution

The general treatment of Sec. III A applies to an arbitrary statistical distribution of the input noise $\eta(t)$ and thus allows a direct examination of the influence of this distribution on stochastic resonance in static nonlinearities. We will not address here the problem of the determination of the optimal noise distribution to maximize stochastic resonance in given conditions, but rather we shall provide an illustration of the explicit influence of the noise distribution that complements the results of Fig. 4. For this purpose, we return to the two-threshold nonlinearity of Eq. (37). With the sinusoidal peri-

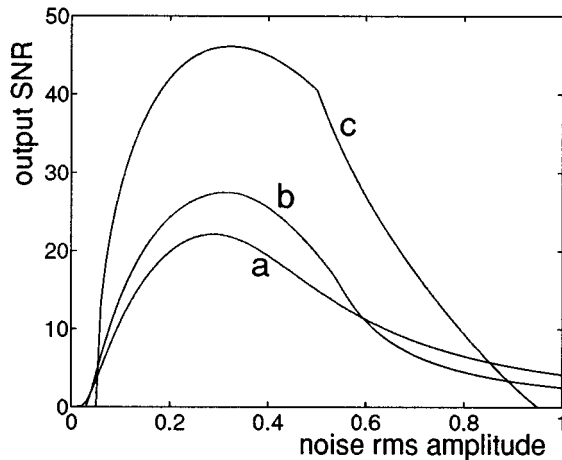


FIG. 11. Influence of the noise distribution. Output signal-to-noise ratio \mathcal{R} at frequency $1/T_s$ computed from Eqs. (31), (38), and (39), for the two-threshold nonlinearity of Eq. (37), as a function of the rms amplitude of the zero-mean input white noise $\eta(t)$, with the periodic input $s(t) = A \sin(2\pi t/T_s)$ and $A = 0.45$. *a*, $\eta(t)$ a Gaussian noise; *b*, $\eta(t)$ a uniform noise; and *c*, $\eta(t)$ a two-level symmetric discrete noise.

odic input $s(t) = A \sin(2\pi t/T_s)$, the results of Fig. 4 show that the uniform noise leads to a higher maximum output SNR compared to the Gaussian noise with the same rms amplitude. Without proving the optimal noise distribution, in this case, we shall show that it is possible to do better than the uniform noise.

Let us consider the family of noise distributions for $\eta(t)$ obtained by passing a zero-mean unit-variance Gaussian noise $\xi(t)$ through the transformation $\eta = A_\eta \tanh(\beta\xi)$ parametrized by A_η and β . For small β 's, the density of η tends to concentrate around zero, qualitatively like a Gaussian density, and with such a shape the noise $\eta(t)$ performs qualitatively like the Gaussian noise for the SNR in stochastic resonance. For intermediate β 's, the density of η tends to be uniform in $[-A_\eta, A_\eta]$, and with such a shape the noise $\eta(t)$ performs qualitatively like the uniform noise for the SNR in stochastic resonance. For large β 's, the density of η tends to concentrate around the two modes $-A_\eta$ and A_η , and with such a shape the noise $\eta(t)$ generally performs better than the uniform noise for the SNR in stochastic resonance. A simple illustration can be obtained for the limit case $\beta \rightarrow +\infty$ where the noise $\eta(t)$ degenerates into a two-level symmetric discrete noise with the density $f_\eta(u) = 0.5[\delta(u + A_\eta) + \delta(u - A_\eta)]$ and rms amplitude A_η . The corresponding distribution function $F_\eta(u)$ is readily written and substituted into Eqs. (38) and (39) to yield the SNR of Eq. (31). This SNR is represented in Fig. 11 and compared to the SNRs of Fig. 4. The results of Fig. 11 show that, in general, neither Gaussian nor uniform noise is optimal to maximize the SNR in stochastic resonance with static nonlinearities. Continuing with the two-level discrete noise on the two-threshold nonlinearity of Eq. (37), it can be shown, with a slight change in the periodic input $s(t)$, that multiple resonant peaks can be obtained for the SNR in stochastic resonance with static nonlinearities, as illustrated in Fig. 12.

G. Output SNR versus input SNR

An important issue is to determine whether stochastic resonance, under given conditions, is able to deliver an out-

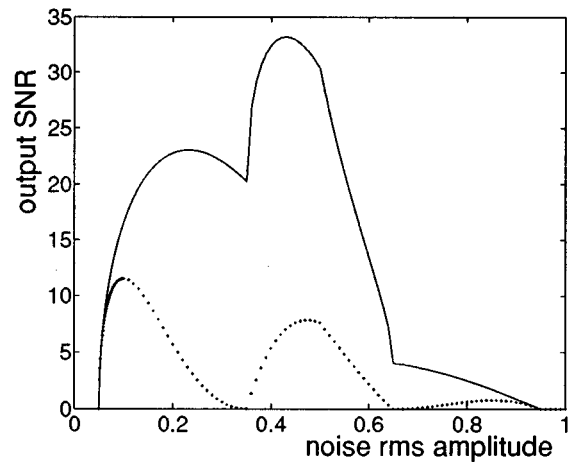


FIG. 12. Multiple resonant peaks. Output signal-to-noise ratio \mathcal{R} computed from Eqs. (31), (38), and (39), for the two-threshold nonlinearity of Eq. (37), as a function of the rms amplitude of the zero-mean two-level symmetric discrete input white noise $\eta(t)$, with the periodic input $s(t) = A \sin(2\pi t/T_s) + 0.15$ and $A = 0.3$. The solid line is \mathcal{R} at frequency $1/T_s$ and the dotted line \mathcal{R} at frequency $2/T_s$.

put SNR larger than the input SNR. Relatively few studies provide clear-cut answers on this issue. For bistable nonlinear dynamic systems, the question is addressed in [38–40]. In the small-signal limit with Gaussian noise, proofs are given in [9,41] that the output SNR cannot exceed that at the input. Under different conditions and with a definition of the SNR differing from the conventional SNR we are considering here, the study in [29] comes to a larger SNR at the output than at the input. We shall now show that, with stochastic resonance in static nonlinearities, the classical SNR defined in Sec. II can be found larger at the output than at the input. Again, we do not plan to elucidate here, in generality, the conditions under which this important property can be obtained. Rather, we will simply produce an illustrative example of its realization.

We consider the periodic input $s(t) = A \sin(2\pi t/T_s)$ with total power $A^2/2$ and power spectral density $P_{ss}(\nu) = A^2[\delta(\nu + 1/T_s) + \delta(\nu - 1/T_s)]/4$, since we chose in this study, according to Eqs. (7) and (8), to represent the spectral distribution of the power with a bilateral power spectral density. $s(t)$ is corrupted by the white noise $\eta(t)$ with autocorrelation function $R_{\eta\eta}(\tau) = 2D\delta(\tau)$ and power spectral density $P_{\eta\eta}(\nu) = 2D$, as introduced in Sec. III A. The input SNR, with the definition of Sec. II, can be expressed as

$$\mathcal{R}_{\text{in}} = \frac{A^2/4}{2D\Delta B}. \quad (48)$$

As explained in Sec. III A, the ideal white noise is realized by a discrete-time noise, with a finite variance σ_η^2 related to the power density $2D$ of the white noise by Eq. (18). The input SNR of Eq. (48) thus becomes

$$\mathcal{R}_{\text{in}} = \frac{(A/\sigma_\eta)^2}{4\Delta t \Delta B}. \quad (49)$$

The output SNR of Eq. (31), at frequency $1/T_s$,

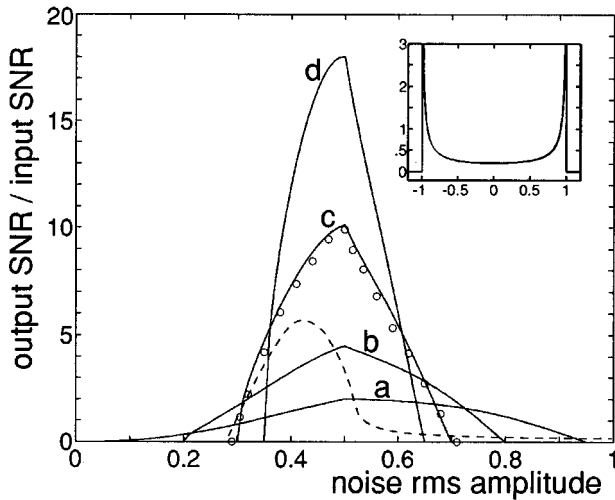


FIG. 13. Output SNR over input SNR $\mathcal{R}_{\text{out}}/\mathcal{R}_{\text{in}}$, as a function of the rms amplitude σ_η of the input white noise $\eta(t)$, with the two-threshold nonlinearity of Eq. (37) and the periodic-input $s(t) = A \sin(2\pi t/T_s)$. With $\eta(t)$ a zero-mean two-level symmetric discrete noise, the four solid curves represent the theoretical expression of Eq. (51), with a , $A=0.45$; b , $A=0.3$; c , $A=0.2$; and d , $A=0.15$, and the discrete data points (open circles) are obtained for the case c from a numerical simulation of the system. The dashed curve is $\mathcal{R}_{\text{out}}/\mathcal{R}_{\text{in}}$ of Eq. (51) with $A=0.15$ when $\eta = A_\eta \tanh(2\xi)$, with ξ a zero-mean unit-variance Gaussian noise and the resulting probability density $f_\eta(u)$ of η shown in the inset as a function of the abscissa u/A_η .

$$\mathcal{R}_{\text{out}} = \frac{|\bar{Y}_1|^2}{\text{var}(y)\Delta t \Delta B}, \quad (50)$$

leads to the ratio

$$\frac{\mathcal{R}_{\text{out}}}{\mathcal{R}_{\text{in}}} = 4 \frac{|\bar{Y}_1|^2 / \text{var}(y)}{A^2 / \sigma_\eta^2}. \quad (51)$$

For the choice of the distribution of the input noise $\eta(t)$, we return to the family of noises $\eta = A_\eta \tanh(\beta\xi)$ of Sec. III F. Finite values of β sufficiently above 1 are adequate to observe the effect, but for a simple illustration we shall again consider the limit case $\beta \rightarrow +\infty$, which gives a two-level symmetric discrete noise $\eta(t)$ of density $f_\eta(u) = 0.5[\delta(u+A_\eta) + \delta(u-A_\eta)]$. Also, as in Sec. III F, we choose the two-threshold nonlinearity of Eq. (37).

With Eqs. (38) and (39), we computed the ratio $\mathcal{R}_{\text{out}}/\mathcal{R}_{\text{in}}$ of Eq. (51), which is represented in Fig. 13, for different values of the amplitude A of the periodic input. A comparison is also given in Fig. 13 with a numerical simulation of the system, which shows, as in Sec. III B, perfect agreement with the theory. The results of Fig. 13 reveal that the ratio $\mathcal{R}_{\text{out}}/\mathcal{R}_{\text{in}}$ resonates with the input noise rms amplitude, although peaking at a slightly higher noise level than the output SNR shown in Fig. 11(c) for $A=0.45$. The curves of Fig. 13 also clearly demonstrate the possibility of an output SNR larger than the input SNR. For very small A 's it is even possible to obtain $\mathcal{R}_{\text{out}} \gg \mathcal{R}_{\text{in}}$.

For the case of a two-level discrete noise $\eta(t) \in \{-A_\eta, A_\eta\}$, as pointed out in [41], there exists a scheme allowing a perfect recovery of $s(t)$ from the mixture

$s(t) + \eta(t)$, provided that the amplitude A of $s(t)$ verifies $A < A_\eta$. Simply, if the measurement is $z = s + \eta > 0$, then s is recovered as $s = z - A_\eta$, and if $z = s + \eta < 0$, then s is recovered as $s = z + A_\eta$. This represents another (nonlinear) recovering scheme that achieves an infinite input-output gain in the SNR, but does not hinder the fact that the stochastic resonator is able to achieve a gain larger than unity. This simple scheme is, however, limited by the condition of $A < A_\eta$, while the stochastic resonator is not and is able to realize $\mathcal{R}_{\text{out}}/\mathcal{R}_{\text{in}} > 1$ also when $A > A_\eta$, as visible in Fig. 13. Moreover, the stochastic resonator is also able to realize $\mathcal{R}_{\text{out}}/\mathcal{R}_{\text{in}} > 1$ when the noise $\eta(t)$ ceases to be a two-level discrete noise, as illustrated in Fig. 13 by $\eta = A_\eta \tanh(2\xi)$, which approaches a uniform noise. In fact, the present theory has the ability to show that a SNR gain larger than unity is not a rare outcome with stochastic resonance in static nonlinearities and it can even be obtained with Gaussian noise when the periodic input is no longer a sinusoid, but we leave this for another study.

H. Stochastic resonance at zero frequency

The expression of the SNR of Eq. (31) of the general model is in principle valid at any harmonic n/T_s of the coherent periodic input, especially for $n=0$. This allows us to investigate the possibility of stochastic resonance at zero frequency. We will consider a situation where both an actual observation and a meaningful interpretation can be given for this extension of stochastic resonance, at zero frequency.

Consider the periodic input $s(t) = A \sin(2\pi t/T_s)$ whose wave form is symmetric relative to the time axis, superposed to an input noise $\eta(t)$ with an even density $f_\eta(u)$. These two inputs are transmitted by the two-threshold nonlinearity of Eq. (37), which is an odd function $g(u)$. In this situation, because of the symmetries of both the inputs $s(t)$ and $\eta(t)$ and the system $g(u)$, the output expectation $E[y(t)]$ averaged over one period T_s , i.e., the quantity \bar{Y}_0 of Eq. (2), will be zero. Indeed, because of the symmetry of $s(t)$, for any time t_1 in $[0, T_s[$, there always exists a time t_2 in $[0, T_s[$ such that $s(t_2) = -s(t_1)$; because of the symmetries of both $f_\eta(u)$ and $g(u)$, the expectations of Eq. (21) verify $E[y(t_2)] = -E[y(t_1)]$ and thus cancel in pairs over one period to yield a zero time-averaged expectation \bar{Y}_0 . In such a case, the SNR at zero-frequency, $\mathcal{R}(0)$ of Eq. (31), is also identically zero for any value of the input noise rms amplitude.

We now consider adding a constant component s_0 to the periodic input, which becomes $s(t) = s_0 + A \sin(2\pi t/T_s)$. The dc component s_0 breaks the symmetry of the periodic input, which is enough to make \bar{Y}_0 differ from zero, with the assurance that any departure of \bar{Y}_0 from zero has its origin in the presence of the input dc component s_0 . One can be interested in performing an estimation of \bar{Y}_0 at the output, in order to extract information on the presence of s_0 at the input. This estimation can be assisted by a stochastic resonance effect, in which an optimum level of the input noise $\eta(t)$ maximizes the time-averaged output mean \bar{Y}_0 relative to the output fluctuations measured by the time-averaged variance $\text{var}(y)$. This is attested by the output SNR at zero frequency $\mathcal{R}(0)$ computed from Eqs. (31), (38), and (39), represented in Fig. 14. Also, the time-averaged output mean \bar{Y}_0

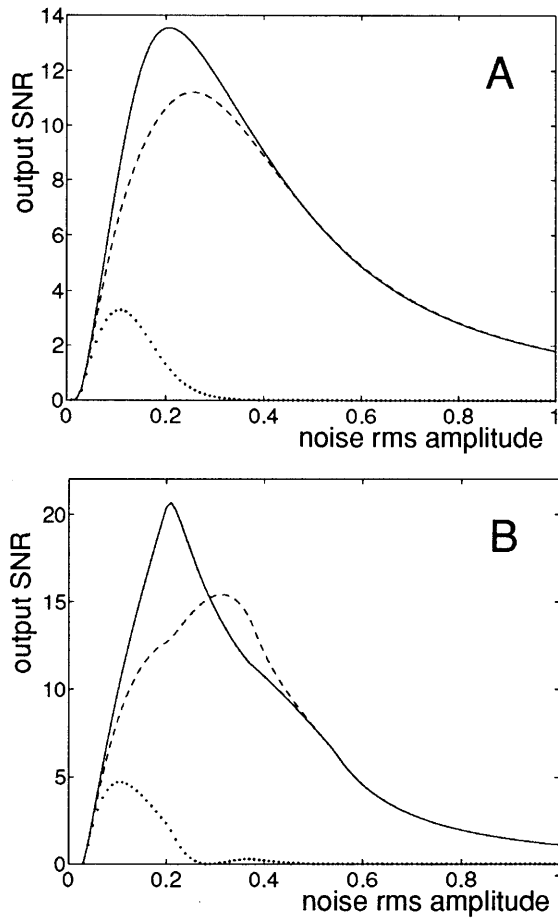


FIG. 14. SNR at zero frequency. Output signal-to-noise ratio \mathcal{R} computed from Eqs. (31), (38), and (39) for the two-threshold nonlinearity of Eq. (37), as a function of the rms amplitude of the input white noise $\eta(t)$. The periodic input is $s(t) = s_0 + A \sin(2\pi t/T_s)$, with $A = 0.3$ and $s_0 = 0.15$. (A) $\eta(t)$ a zero-mean Gaussian noise and (B) $\eta(t)$ a zero-mean uniform noise. In each panel, the solid line is the SNR $\mathcal{R}(0)$ at zero frequency, the dashed line is $\mathcal{R}(1/T_s)$, and the dotted line is $\mathcal{R}(2/T_s)$.

alone undergoes, like the SNR $\mathcal{R}(0)$, a nonmonotonic variation with the input noise rms amplitude, as visible in Fig. 15.

It is also possible to obtain stochastic resonance at zero frequency when the periodic input degenerates into a simple constant $s(t) = s_0 \forall t$. The issue of stochastic resonance with a constant coherent input has been addressed in [42,43] for multistable nonlinear dynamic systems as discussed in Sec. I. Here, for static nonlinear systems, we shall demonstrate that a form of stochastic resonance can be observed with a constant coherent input. A constant input is a special case of a periodic input and the uniform mode of calculation that has been used throughout the present study can be kept in this case, with any finite value of T_s for the period of the constant $s(t)$, to perform the time averages as in Eqs. (2), (6), (28), or (26). But, of course, with a constant $s(t)$ the results are no different if these time averages are simply not performed. The SNR of Eq. (31) at zero frequency, in this case, can be computed as

$$\mathcal{R}(0) = \frac{E^2(y)}{\text{var}(y) \Delta t \Delta B} \quad (52)$$

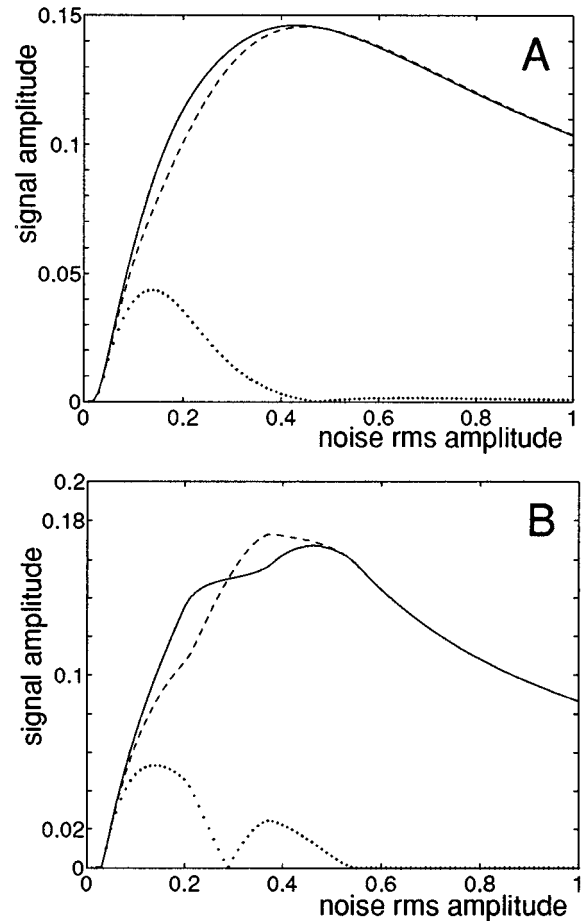


FIG. 15. Output coherent signal amplitude $|\bar{Y}_n|$ at frequency n/T_s computed from Eqs. (28) and (38) for the two threshold nonlinearity of Eq. (37), as a function of the rms amplitude of the input white noise $\eta(t)$. The periodic input is $s(t) = s_0 + A \sin(2\pi t/T_s)$, with $A = 0.3$ and $s_0 = 0.15$. (A) $\eta(t)$ a zero-mean Gaussian noise and (B) $\eta(t)$ a zero-mean uniform noise. In each panel, the solid line is \bar{Y}_0 at zero frequency, the dashed line is $|\bar{Y}_1|$ at $1/T_s$, and the dotted line is $|\bar{Y}_2|$ at $2/T_s$.

and is represented in Fig. 16 together with the output mean $E(y)$ from Eq. (38), for the two-threshold nonlinearity of Eq. (37).

Equation (52) shows that $\sqrt{\mathcal{R}(0)}$ is simply proportional to $E(y)/\sqrt{\text{var}(y)}$, which is interpretable as the relative accuracy in estimating the constant $E(y)$ embedded in fluctuations with rms amplitude $\sqrt{\text{var}(y)}$. The nonmonotonic variation of $\sqrt{\mathcal{R}(0)}$ with the input noise level, as it follows from Fig. 16(B) indicates that there is an optimal level where the estimation of the constant $E(y)$ can be performed with best accuracy. In other words, there is an optimal input noise level where the value of the output mean $E(y)$ is maximized relative to the rms output fluctuation $\sqrt{\text{var}(y)}$. If we return to the strictly periodic, nonconstant, input $s(t) = s_0 + A \sin(2\pi t/T_s)$, for instance, a similar interpretation is valid for the resonant $\sqrt{\mathcal{R}(0)}$ from Fig. 14, as proportional to the relative accuracy in estimating the time-averaged output mean $E(y) = \bar{Y}_0$ embedded in output fluctuations with time-averaged rms amplitude $\sqrt{\text{var}(y)}$.

If the model of the process is known, especially $f_\eta(u)$ and

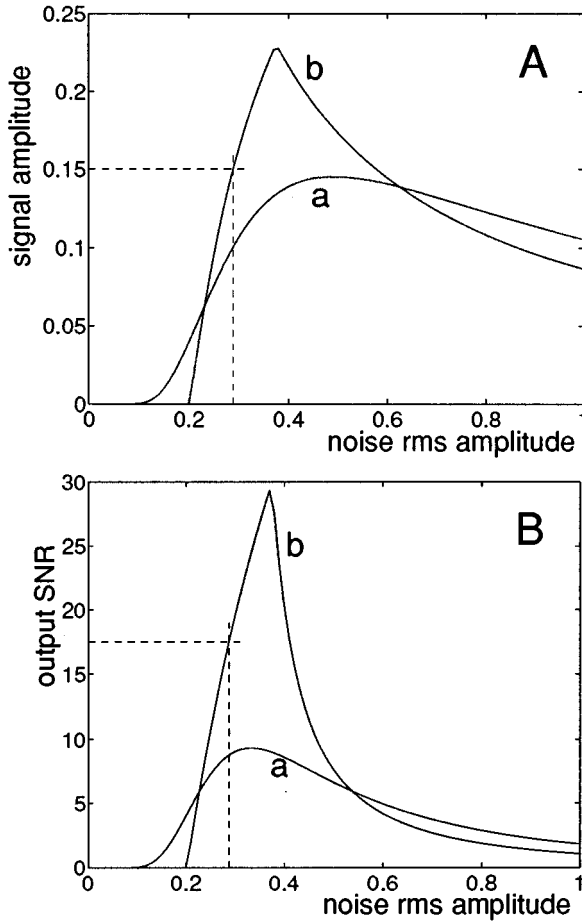


FIG. 16. Two-threshold nonlinearity of Eq. (37) with a constant coherent input $s(t) = s_0 \forall t$ with $s_0 = 0.15$. (A) Output coherent signal amplitude $Y_0 = E(y)$ at zero frequency from Eq. (38) and (B) output signal-to-noise ratio $\mathcal{R}(0)$ at zero frequency from Eqs. (52) and (39), both as a function of the rms amplitude σ_η of the input white noise $\eta(t)$. In each panel, *a* is with $\eta(t)$ a zero-mean Gaussian noise and *b* with $\eta(t)$ a zero-mean uniform noise. On the curves *b* with the uniform noise, where the two dashed lines meet is the location of the optimal dithering, at $\sigma_\eta = 0.5/\sqrt{3} \approx 0.29$, corresponding to $\eta(t)$ uniform over $[-0.5, 0.5]$, which allows one to obtain $E(y) = s_0$ (A), but with a SNR and thus a performance of estimation of $E(y)$, which is not optimal (B).

$g(u)$, the knowledge of the output mean $\overline{E(y)}$ will usually allow one, through the use of a calculable calibration curve, to recover the input mean s_0 . An accurate estimation of $\overline{E(y)}$ obtained at the maximum of the output SNR $\mathcal{R}(0)$ is thus desirable to an accurate estimation of s_0 .

Stochastic resonance at zero frequency leads thus to the possibility of maximizing, with an optimal input noise level, the ratio of the time-averaged output mean $\overline{E(y)} = \overline{Y}_0$ to the time-averaged output fluctuations $\sqrt{\text{var}(y)}$. This property of stochastic resonance at zero frequency can be related to the dithering effect [20]. Dithering takes place with static threshold nonlinearities intervening in analog-to-digital conversion of a coherent signal $s(t)$ added to a noise $\eta(t)$. For the two-threshold nonlinearity $g(u)$ of Eq. (37), optimal dithering is achieved by an input noise $\eta(t)$ uniform over $[-0.5, 0.5]$. As it can be verified from Eq. (38), optimal dithering leads to $\overline{E[y(t)]} = s(t)$, when $-0.5 \leq s(t) \leq 0.5$. In

other words, optimal dithering allows the time-averaged output mean $\overline{E[y(t)]}$ to reproduce the mean value $s(t)$ of the periodic input. This is the very property that is sought with dithering. Dithering can now be contrasted with stochastic resonance at zero frequency. Briefly, dithering is an output mean that reproduces the input mean, while stochastic resonance is an output mean that stands out maximally off the output fluctuations. However, as visible in Fig. 16, the input noise level that optimizes dithering, i.e., that realizes $\overline{E[y(t)]} = s(t)$, is usually not the same as the noise level that maximizes $\overline{E[y(t)]} / \sqrt{\text{var}[y(t)]}$, i.e., that maximizes the SNR $\mathcal{R}(0)$. The accuracy of a statistical estimation of $\overline{E[y(t)]}$ will generally be better at the maximum of stochastic resonance than at the optimal dithering.

I. Discussion of static nonlinearities with white noise

The discrete-time treatment of Sec. III A with a time step Δt is exact for any physically realizable “white” noise $\eta(t)$ endowed with a correlation time τ_c smaller than the time resolution Δt . If the correlation of the noise $\eta(t)$ strictly vanishes above Δt , then all the numerical quantities theoretically defined in Sec. III A exactly match, in principle, the corresponding quantities experimentally measurable in any physical implementation of the process. This was verified in the experiment reported in Sec. III B, at least within the accuracy of the experimental measurements and also in the computer experiments of the simulations of Fig. 13 and [22].

Our modeling choice to handle the white-noise case is thus to develop a discrete-time treatment together with the consideration of a physical white noise defined by a correlation time smaller than the time resolution of the discrete-time treatment. Additionally, the discrete-time treatment has the advantage of yielding expressions that can be computed in the same way in a theoretical analysis, a computer simulation, and an experimental implementation. In particular, this modeling strategy renders unnecessary the prior realization of filtering procedures aimed at taming undesirable pathologies attached to an ideal white noise, such as infinite variance or infinite zero-crossing rate, and as they are used in [19,18]. In physical situations, these pathologies do not exist in the first place because the white noise $\eta(t)$ will have a short but finite correlation time. In the following section we shall consider the case of a nonvanishing correlation time of the input noise $\eta(t)$ that has to be explicitly taken into account.

IV. STATIC NONLINEARITIES WITH COLORED NOISE

We now consider the same static nonlinearity of Eq. (16), but when the stationary noise $\eta(t)$ is colored. The output expectation introduced in Eq. (3) can then be evaluated under the form

$$E[y(t)y(t+\tau)] = \int_{-\infty}^{+\infty} \int_{-\infty}^{+\infty} g(u_1)g(u_2)f_{\eta\eta}[u_1-s(t), u_2 - s(t+\tau); \tau] du_1 du_2, \quad (53)$$

where $f_{\eta\eta}(u_1, u_2; \tau)$ is the second-order probability density function of the stationary noise $\eta(t)$.

When $f_{\eta\eta}(u_1, u_2; \tau)$ is known for the input noise $\eta(t)$, then the general scheme described in Sec. II can be explicitly

realized, possibly with the aid of numerical integrations. After evaluation of $E[y(t)y(t+\tau)]$ through Eq. (53), a time average over t has to be performed according to Eq. (4) to obtain the autocorrelation function $R_{yy}(\tau)$ whose Fourier transform yields the power spectral density $P_{yy}(\nu)$ appropriate to evaluate the output SNR \mathcal{R} . The input-output phase shift ϕ of Eq. (15) is evaluated without additional difficulty, from Eqs. (21) and (2), since this requires only the first-order probability density $f_{\eta}(u)$ of the colored input noise $\eta(t)$.

The exact computation of the output SNR with a static nonlinearity and a colored noise thus requires, in general, the knowledge of the second-order probability density $f_{\eta\eta}(u_1, u_2; \tau)$ of the input noise. It is seldom the case that such a multivariate function is known for a random noise $\eta(t)$. What is much more common in practice is the sole knowledge of the single-variable autocorrelation function $R_{\eta\eta}(\tau) = E[\eta(t)\eta(t+\tau)]$ of the stationary noise $\eta(t)$. In general, with an arbitrary nonlinearity $g(u)$, the knowledge of $R_{\eta\eta}(\tau)$ is not sufficient for the exact evaluation of the output expectation of Eq. (53), which opens the way to the complete characterization of the SNR in stochastic resonance. However, the knowledge of $R_{\eta\eta}(\tau)$ will suffice in a special case, which is often met in practice, when $\eta(t)$ is a Gaussian noise, since in this case $f_{\eta\eta}(u_1, u_2; \tau)$ is completely defined once $R_{\eta\eta}(\tau)$ is given [35].

To circumvent this difficulty originating in the usually limited knowledge of the second-order statistics of the colored input noise, we shall now propose an approximation that renders possible an evaluation of the output SNR based only on the knowledge of the input autocorrelation function $R_{\eta\eta}(\tau)$. We introduce the autocovariance function of the input noise $\eta(t)$ as $C_{\eta\eta}(\tau) = R_{\eta\eta}(\tau) - R_{\eta\eta}(+\infty) = R_{\eta\eta}(\tau) - E^2(\eta)$. For a colored noise $\eta(t)$, the autocovariance $C_{\eta\eta}(\tau)$ is a symmetric pulse concentrated around the origin, which goes to zero when $|\tau| \rightarrow +\infty$. The extension of this pulse around $\tau=0$ can be measured with a correlation time τ_c , which estimates the duration over which $\eta(t)$ keeps significant correlation. A key point then is that we are in the presence of a static nonlinearity $g(u)$, whose output $y(t)$ is only influenced by the instantaneous value of $s(t) + \eta(t)$. It is then natural to admit that the autocovariance function $C_{yy}(\tau)$ of the output signal $y(t)$ as defined by Eq. (6), will also be a pulse extending around the origin over a duration of order τ_c . Equation (11) shows that both the magnitude of the autocovariance $C_{yy}(0) = \overline{\text{var}[y(t)]}$ and its normalized shape $h(\tau) = C_{yy}(\tau)/C_{yy}(0)$ via $H(\nu)$ influence the output SNR. The magnitude $C_{yy}(0) = \overline{\text{var}[y(t)]}$ is a first-order statistical quantity that can be computed, with a static $g(u)$, only with the knowledge of first-order statistics of the input noise $\eta(t)$, through Eq. (23). After normalization by the factor $C_{yy}(0)$, which is exactly computable with first-order statistics, the normalized output autocovariance $h(\tau) = C_{yy}(\tau)/C_{yy}(0)$ that remains will display a pulselike shape of duration $\sim \tau_c$ just like the normalized input autocovariance $C_{\eta\eta}(\tau)/C_{\eta\eta}(0)$. The form of $h(\tau)$ can be taken as a distorted version of $C_{\eta\eta}(\tau)/C_{\eta\eta}(0)$. Only in a few simple situations can $h(\tau)$ be explicitly deduced from $C_{\eta\eta}(\tau)/C_{\eta\eta}(0)$. This is the case, for instance, with a Gaussian $\eta(t)$, no periodic modulation $s(t)$, and a signum function for $g(u)$, with Price's theorem and the arcsine law [35]. An explicit expression for $h(\tau)$ is much more difficult to obtain in the presence of the periodic

modulation $s(t)$; when the Gaussian assumption breaks down, as mentioned, $C_{\eta\eta}(\tau)/C_{\eta\eta}(0)$ or $R_{\eta\eta}(\tau)$ are insufficient for an exact expression of $h(\tau)$. Based on the properties that we have explained, for $h(\tau)$ in the presence of a static nonlinearity, we propose to use the simple approximation

$$h(\tau) \approx \frac{C_{\eta\eta}(\tau)}{C_{\eta\eta}(0)}. \quad (54)$$

In this approximation scheme, in the evaluation of the output autocovariance $C_{yy}(\tau)$, which controls the denominator of the output SNR of Eq. (11), only the exact magnitude of $C_{yy}(\tau)$ measured by $C_{yy}(0) = \text{var}[y(t)]$ is exactly monitored. The normalized shape $h(\tau)$ of $C_{yy}(\tau)$ is simply approximated, through Eq. (54), which amounts to neglecting the distortion introduced in the normalized autocovariance by the static nonlinearity $g(u)$. If the SNR of Eq. (11) is expressed in decibels in the form

$$\mathcal{R}\left(\frac{n}{T_s}\right) = 10 \log_{10} \left(\frac{|\bar{Y}_n|^2}{\text{var}[y(t)]} \right) - 10 \log_{10} [H(n/T_s) \Delta B], \quad (55)$$

then the first term on the right-hand side is exactly computable with first-order statistics on the input noise through Eq. (23), while the second term will only be approximated from Eq. (54).

A further plausible expectation reinforcing the usefulness of the present approximation appears when we come to the examination of the variation of the output SNR with the input noise power. The normalized output autocovariance $h(\tau)$, whether or not it is well approximated by Eq. (54), may be expected to display relatively little variation with the input noise power, with a static nonlinearity and after the normalization, in comparison to the variations of $\overline{\text{var}[y(t)]}$ in Eq. (55) that alone are responsible for the resonance with white noise. The normalized autocovariance $C_{\eta\eta}(\tau)/C_{\eta\eta}(0)$ at the input does not change with the input noise power, and we simply admit that this is also true, approximately, for $h(\tau)$ at the output. In this way, the approximation of Eq. (54) may possibly lead to a loose approximation of the SNR in Eq. (55), but this approximation may be expected to be satisfactory within an additive constant, and for this reason appropriate to yield a representation of the variations of the SNR with the input noise power and especially to estimate the noise level that produces the maximum SNR.

The validity of the present approximation scheme has been tested with a very common correlation structure for the colored noise $\eta(t)$, namely, when $\eta(t)$ is Gaussian and exponentially correlated with the autocorrelation function

$$R_{\eta\eta}(\tau) = \frac{D}{\tau_c} \exp\left(-\frac{|\tau|}{\tau_c}\right) \quad (56)$$

and the power spectral density $P_{\eta\eta}(\nu) = 2D/[1 + (2\pi\tau_c\nu)^2]$. The theoretical SNR of Eq. (55) has been computed with the approximation resulting from Eq. (54) for $H(\nu) = \mathcal{F}[h(\tau)]$. This theoretical SNR is compared in Fig. 17 with the experimental SNR resulting from a numerical simulation of the nonlinear system.

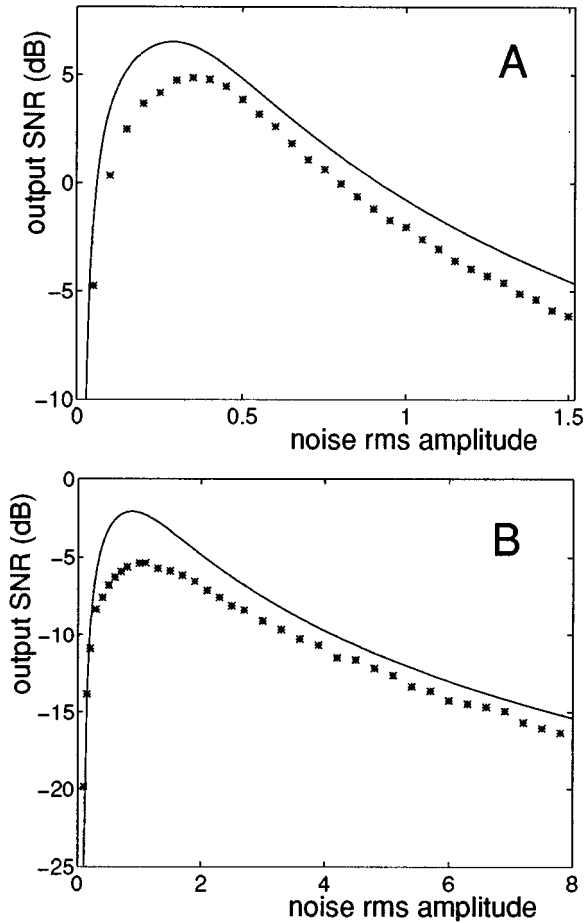


FIG. 17. Output signal-to-noise ratio $\mathcal{R}(1/T_s)$ in decibels, as a function of the rms amplitude of the Gaussian input colored noise $\eta(t)$ with the exponential correlation of Eq. (56) and the coherent periodic input $s(t) = A \sin(2\pi t/T_s)$. The solid line is the theoretical approximation of the SNR from Eqs. (55) and (54) and the discrete data points represent the experimental SNR resulting from a numerical simulation of the nonlinear system. (A) Two-threshold nonlinear system of Eq. (37), a coherent amplitude $A = 0.45$, and a noise correlation time $\tau_c = T_s$. (B) Diode nonlinearity of Eq. (42) with $\theta = 1.2$, $\lambda = 1$, a coherent amplitude $A = 1$, and a noise correlation time $\tau_c = T_s/2$.

The results of Fig. 17 show that the approximation of Eq. (54) is able to provide a satisfactory estimation of the output SNR. In detail, the quality of the approximation is influenced by the type of the periodic input $s(t)$ and that of the nonlinearity $g(u)$ and by the correlation structure of the noise $\eta(t)$, especially its correlation time τ_c . However, in general, the approximation scheme of Eq. (54) is able to predict the existence of stochastic resonance and to offer estimations for both the SNR values and the input noise rms amplitude yielding the maximum of the resonance.

The approximation scheme of Eq. (54) is tested in Fig. 17 for a noise correlation time τ_c of the same order of magnitude as the coherent period T_s . This approximation scheme can also be applied when $\tau_c \gg T_s$, but in this case, the noise with its frequency content up to $\sim 1/\tau_c$ will have practically no power in the region $1/T_s \gg 1/\tau_c$ of the coherent signal, making stochastic resonance of little use since the signal at $1/T_s$ strongly dominates the noise. On the other hand, for

$\tau_c \ll T_s$ the white-noise treatment of Sec. III is expected to yield a correct approximation. For $\tau_c \sim T_s$, the approximation of Eq. (54) offers a simple and general scheme, which may be the only one of its kind, readily and practically applicable, when the Gaussian hypothesis does not hold and the knowledge of the second-order statistics of the input noise $\eta(t)$ is limited to the autocorrelation function $R_{\eta\eta}(\tau)$.

V. EXTENSION OF THE DOMAIN OF APPLICABILITY

The present theory, which allows the characterization of a stochastic resonance effect, applies to static nonlinear systems of the form of Eq. (16). However, the domain of applicability of this theory can readily be extended to dynamic nonlinear systems that can be decomposed into a static nonlinearity of the form (16) followed by an arbitrary linear dynamic system. Indeed, a linear dynamic system on the output of a static nonlinearity (16) only multiplies the output power spectral density $P_{yy}(\nu)$ by a fixed function of the frequency ν , the squared modulus of the transfer function of the linear dynamic system [35]. As a result, the SNR as defined in the present study will be no different if evaluated at the output of the linear system, since the spectral line and the noise background at a given frequency are multiplied by the same constant. The input-output phase shift, at a given frequency, will simply be changed by the constant phase shift added by the linear system at this frequency. In this way, for any nonlinear dynamic system formed by a static nonlinearity followed by a linear dynamic system, the property of stochastic resonance can be characterized by the sole examination of the transfer by the static nonlinearity and the performance of the resonance in the transfer by the whole system is equivalent to that in the transfer by the sole static nonlinearity.

This extension of the domain of applicability of the present theory allows one to annex to its realm nonlinear systems that would have been categorized in the class of excitable systems as discussed in Sec. I rather than static nonlinear systems. Consider, for instance, a periodic input plus noise compared to a threshold to generate a stereotypical output pulse each time the threshold is crossed: a positive pulse for an upward crossing and a negative pulse for a downward crossing. This excitable system can be reproduced with a Heaviside static nonlinearity with the same threshold and receiving the periodic input plus noise. A derivation is then performed on its output to yield a train of Dirac δ pulses at the locations of the threshold crossings. This train is then convolved with a kernel representing the stereotypical pulse. Since both the derivation and convolution are linear operations, the stochastic resonance will occur in the same conditions at the output of the whole excitable system and at the output of the Heaviside nonlinearity. In particular, the resonance will be unaffected by the shape of the stereotypical pulse.

VI. CONCLUSION

A theory has been developed that is able to describe the property of noise-enhanced signal transmission through stochastic resonance in a broad class of nonlinear systems. This theory applies to any nonlinear dynamic system that can be

decomposed into a static nonlinearity followed by an arbitrary linear dynamic system. The possibility of such a general theory certainly relates to the separation between the nonlinear and the dynamic characters of the systems: the nonlinear part is static and the dynamic part is linear. This contrasts the present theory with other approaches to stochastic resonance (see Sec. I) that deal with systems where the nonlinear and dynamic characters are tightly mixed. The static character of the present nonlinearities allows a direct statistical analysis, in which all the quantities relevant to characterize stochastic resonance in the output signal can be obtained from statistics computed directly on the input noise.

The theory shows that, with static nonlinearities, stochastic resonance can be characterized, exactly with white noise and approximately with colored noise, by monitoring only first-order statistical properties of the output signal $y(t)$. The essential quantities are the nonstationary output mean $E[y(t)]$ and the time-averaged output variance $\overline{\text{var}[y(t)]}$. Stochastic resonance with static nonlinearities can thus be seen as a redistribution of power (first-order statistics) rather than a redistribution of correlation (second-order statistics) between the noise and the coherent part in the output signal.

For the case of white input noise, the theory offers an

exact description in a discrete-time framework directly confrontable to experiments or simulations. Reported experiments and simulations strongly support the theory.

The theory was used to demonstrate a wide range of interesting effects in static nonlinearities such as stochastic resonance with nonsinusoidal periodic inputs and non-Gaussian noises; stochastic resonance with nonsubliminal periodic inputs and monotonic or nonmonotonic smooth nonlinearities; multiple resonant peaks in the SNR and nonzero input-output phase shifts; and a SNR larger at the output than at the input. The theory has demonstrated stochastic resonance in a simple diodelike nonlinearity, which offers a possibility for a physical (electronic) implementation of one of the simplest conceivable stochastic resonators. The theory has shown the possibility of stochastic resonance at zero frequency, with a periodic input or with a constant input, and suggested the relation of the known phenomenon of dithering to stochastic resonance at zero frequency. The present theory, offering a general description for a broad class of nonlinear dynamic systems, some of which are very easily experimentally implementable, constitutes a unique framework for further investigations of stochastic resonance and its applications.

-
- [1] R. Benzi, A. Sutera, and A. Vulpiani, *J. Phys. A* **14**, L453 (1981).
- [2] R. Benzi, G. Parisi, A. Sutera, and A. Vulpiani, *Tellus* **34**, 10 (1982).
- [3] C. Nicolis, *Tellus* **34**, 1 (1982).
- [4] F. Moss, A. Bulsara, and M. F. Shlesinger, *Proceedings of the NATO Advanced Research Workshop on Stochastic Resonance in Physics and Biology* [*J. Stat. Phys.* **70**, 1 (1993)].
- [5] F. Moss, in *Contemporary Problems in Statistical Physics*, edited by G. H. Weiss (SIAM, Philadelphia, 1994), pp. 205–253.
- [6] F. Moss, D. Pierson, and D. O’Gorman, *Int. J. Bif. Chaos* **4**, 1383 (1994).
- [7] K. Wiesenfeld and F. Moss, *Nature* **373**, 33 (1995).
- [8] A. R. Bulsara and L. Gammaitoni, *Phys. Today* **49** (3), 39 (1996).
- [9] M. I. Dykman, D. G. Luchinsky, R. Mannella, P. V. E. McClintock, N. D. Stein, and N. G. Stocks, *Nuovo Cimento D* **17**, 661 (1995).
- [10] L. Gammaitoni, F. Marchesoni, E. Menichella-Saetta, and S. Santucci, *Phys. Rev. Lett.* **62**, 349 (1989).
- [11] P. Jung and P. Hänggi, *Europhys. Lett.* **8**, 505 (1989).
- [12] N. G. Stocks, N. D. Stein, S. M. Soskin, and P. V. E. McClintock, *J. Phys. A* **25**, L1119 (1992).
- [13] N. G. Stocks, N. D. Stein, and P. V. E. McClintock, *J. Phys. A* **26**, L385 (1993).
- [14] M. Gitterman and G. H. Weiss, *J. Stat. Phys.* **70**, 107 (1993).
- [15] K. Wiesenfeld, D. Pierson, E. Pantazelou, C. Dames, and F. Moss, *Phys. Rev. Lett.* **72**, 2125 (1994).
- [16] A. R. Bulsara, S. B. Lowen, and C. D. Rees, *Phys. Rev. E* **49**, 4989 (1994).
- [17] Z. Gingl, L. B. Kiss, and F. Moss, *Europhys. Lett.* **29**, 191 (1995).
- [18] P. Jung, *Phys. Lett. A* **207**, 93 (1995).
- [19] P. Jung, *Phys. Rev. E* **50**, 2513 (1994).
- [20] L. Gammaitoni, *Phys. Rev. E* **52**, 4691 (1995).
- [21] L. Gammaitoni, *Phys. Lett. A* **208**, 315 (1995).
- [22] F. Chapeau-Blondeau, *Phys. Rev. E* **53**, 5469 (1996).
- [23] B. McNamara and K. Wiesenfeld, *Phys. Rev. A* **39**, 4854 (1989).
- [24] G. Hu, H. Haken, and C. Z. Ning, *Phys. Lett. A* **172**, 21 (1992).
- [25] M. I. Dykman, P. V. E. McClintock, R. Mannella, and N. G. Stocks, *JETP Lett.* **52**, 144 (1990).
- [26] M. I. Dykman, R. Mannella, P. V. E. McClintock, and N. G. Stocks, *Phys. Rev. Lett.* **68**, 2985 (1992).
- [27] M. I. Dykman, D. G. Luchinsky, R. Mannella, P. V. E. McClintock, N. D. Stein, and N. G. Stocks, *J. Stat. Phys.* **70**, 463 (1993).
- [28] M. I. Dykman, H. Haken, G. Hu, D. G. Luchinsky, R. Mannella, P. V. E. McClintock, C. Z. Ning, N. D. Stein, and N. G. Stocks, *Phys. Lett. A* **180**, 332 (1993).
- [29] L. B. Kiss, *Proceedings of the Third Technical Conference on Nonlinear Dynamics (Chaos) and Full Spectrum Processing, Mystic, 1995* (AIP, New York, 1995).
- [30] F. Chapeau-Blondeau, X. Godivier, and N. Chambet, *Phys. Rev. E* **53**, 1273 (1996).
- [31] X. Godivier and F. Chapeau-Blondeau, *Europhys. Lett.* **35**, 473 (1996).
- [32] F. Chapeau-Blondeau and X. Godivier, *Int. J. Bif. Chaos* **6**, 2069 (1996).
- [33] J. J. Collins, C. C. Chow, and T. T. Imhoff, *Phys. Rev. E* **52**, R3321 (1995).
- [34] P. Jung and P. Hänggi, *Phys. Rev. A* **44**, 8032 (1991).
- [35] A. Papoulis, *Probability, Random Variables, and Stochastic Processes* (McGraw-Hill, New York, 1991).
- [36] S. Fauve and F. Heslot, *Phys. Lett. A* **97**, 5 (1983).
- [37] X. Godivier and F. Chapeau-Blondeau, *Signal Processing* (to

- be published).
- [38] D. C. Gong, G. Hu, X. D. Wen, C. Y. Yang, G. R. Qin, R. Li, and D. F. Ding, *Phys. Rev. A* **46**, 3243 (1992).
- [39] D. C. Gong, G. Hu, X. D. Wen, C. Y. Yang, G. R. Qin, R. Li, and D. F. Ding, *Phys. Rev. E* **48**, 4862 (1993).
- [40] M. E. Inchiosa and A. R. Bulsara, *Phys. Rev. E* **52**, 327 (1995).
- [41] M. DeWeese and W. Bialek, *Nuovo Cimento D* **17**, 733 (1995).
- [42] M. Gitterman, I. B. Khalfin, and B. Y. Shapiro, *Phys. Lett. A* **184**, 339 (1994).
- [43] J. M. Casado, J. J. Mejias, and M. Morillo, *Phys. Lett. A* **197**, 365 (1995).